

https://dspace.org/

Radiophotoluminescence glass dosimetry end-to-end audit of high dose rate gynaecological brachytherapy in Charlotte Maxeke Johannesburg Academic Hospital

Ntombela, Lethukuthula Nqobizitha

2020

https://hdl.handle.net/10539/30157

Downloaded from a DSpace repository. https://dspace.org/

RADIOPHOTOLUMINESCENCE GLASS DOSIMETRY END-TO-END AUDIT OF HIGH DOSE RATE GYNAECOLOGICAL BRACHYTHERAPY IN CHARLOTTE MAXEKE JOHANNESBURG ACADEMIC HOSPITAL

by

LETHUKUTHULA NQOBIZITHA NTOMBELA

Submitted in partial fulfilment of the requirements for the degree

MASTER OF SCIENCE



SCHOOL OF PHYSICS

2020

Supervisor: Prof. D G van der Merwe

Declaration of authenticity

I declare that the research study, *Radiophotoluminescence glass dosimetry end – to – end audit of high dose rate gynaecological brachytherapy in Charlotte Maxeke Johannesburg Academic Hospital*, is my own work and each source of information used has been acknowledged by means of a complete reference. This thesis has not been submitted before for any other research project, degree or examination at any university.



……..

Signature of student

Date: 20/04/2020

Johannesburg South Africa

(City / town of student's residence

Copyright information

This dissertation/ thesis may not be published either (in scholarly, scientific or technical journals), or as a whole (as a monograph), by the researcher or any other person unless permission has been obtained from University of the Witwatersrand.

I agree that I have read and understand the copyright notice

L.N. Ntombela



……

ABSTRACT

OBJECTIVES: The objective of this research was to verify the correct delivery of the treatment plans used for gynaecological brachytherapy applications in accordance with Charlotte Maxeke Johannesburg Academic Hospital (CMJAH) clinical protocols. Different techniques were employed that included computed doses from the treatment plans, radiophotoluminescence glass dosimeter measurements and Monte Carlo simulations. The main purpose was to develop and implement an end-to-end dosimetry audit in High Dose Rate (HDR) gynaecological brachytherapy, develop an approach for gynaecological brachytherapy audits in South Africa, and improve quality in HDR brachytherapy treatment at CMJAH.

MATERIALS AND METHOD: A water phantom was designed using CAD (Computer Aided Design) software and was manufactured in order to perform Ir-192 HDR brachytherapy absolute-dose measurements in the water around an applicator in a fixed geometry. The applicators were scanned using CT and reconstructed on the CT images and plans were created, using standard clinical protocols at CMJAH. The prescribed dose of 8 Gy at point "A" was used. In this work, the doses calculated by the planning system were compared with the results obtained from the RPLGD and Monte Carlo simulations.

RESULTS: The doses measured by the radiophotoluminescence glass dosimeters were in good agreement with treatment planning calculated doses and Monte Carlo simulated doses. From point "A" to point "B" the overall variation between the measured, calculated and simulated doses was less than 3%. For distances greater than 6 cm from the sagittal center of the applicator shows the deterioration with under response of radiophotoluminescence glass dosimeters compared with treatment planning system.

CONCLUSION: The results of this work have shown that radiophotoluminescence glass dosimeters are capable of dose distribution measurements around gynaecological applicators for the purpose of dosimetric audits in HDR brachytherapy.

Acknowledgements

I would like to thank my supervisor Prof Debbie van der Merwe for the patient guidance, encouragement and advice she has provided throughout this study.

I would also like to thank NMISA to provide access to use their dosimeters and readout system.

I must express my gratitude to Vincent Maselesele for teaching me how the dosimeters and readout system works and Mr. Mathoho for manufacturing the testing water phantom.

Lastly, I would like to thank my wife Palesa for her willingness to proof read some of my work.

Table of Contents

List of figures vii

List of Tables ix

CHAPTER ONE 1

INTRODUCTION 1

1.1. Dosimetry audits 2
1.2. Research objectives 2
1.3. The need for national external audits in brachytherapy 3
1.4. Summary of the Research Project 4

CHAPTER TWO 5

Literature review 5

2.1. Introduction 5
2.2. Radio-photoluminescence glass dosimeters (RPLGDs) 7
2.3. Characteristics of RPLGDs 9
2.4. HDR Brachytherapy 10
2.5. Dose distribution measurements in HDR brachytherapy 12
2.5.1 Brachytherapy treatment-planning system 12
2.6. Monte Carlo technique 14
2.6.1 Monte Carlo simulation research in brachytherapy 14
2.6.2 MCNP code 16

CHAPTER THREE 18

Materials and Methodology 18

3.1. Introduction 18
3.2. Equipment and materials 18
3.3. Method 20
3.3.1. Phantom design 20
3.3.2. RPLGD preparation 25
3.3.3. Determination of dosimeters characteristics 26
3.3.4. Glass dosimeter calibration using a cobalt teletherapy beam 27
3.3.5. RPLGDs position verification 28
3.3.6. CT Scan and planning 29
3.3.7. Treatment delivery 30
3.3.8. Monte Carlo technique 32
3.3.9. The MCNP structure 32
3.3.10. Phantom and Source model 33
3.3.11. Monte Carlo process 34

CHAPTER FOUR 36

RESULTS AND DISCUSSION 36

4.1. Sensitivity correction factor 37
4.2. RPLGD reproducibility 39
4.3. RPLGD linearity response 41
4.4. RPLGD calibration factor using a Cobalt 60 Teletherapy source 42
4.5. RPLGDs position verification using 20 mm diameter sorbo 43
4.6. Absorbed dose (Gy) TPS brachytherapy and RPLGD for ring tube and IU 6 cm applicators 44
4.7. Absorbed dose (Gy) TPS brachytherapy and RPLGD for ovoids tubes and IU 6 cm applicators 45
4.8. Monte Carlo technique 46
4.9. Uncertainty analysis 50
CHAPTER FIVE 52
Conclusions 52
REFERENCES 54
Ethics clearance 59

List of figures

Figure 2.1: The colour centers showing motion mechanism……..……..8
Figure 2.2: The energy levels of RPLGD. (1) After RPLGD being exposed, Ag+ at the valence band combines with electron released from PO4- and hPO4 formed by PO4- to become a colour center. (2) After electron at colour center excited by 337.1 nm pulse ultra- violet laser, it will be excited and emits 600-700 nm visible orange light, then return to the original colour centers. (3) After annealing at 4000C for one hour, the electron at colour centers returns to the valence band of luminescence material (Hsu, 2016).…….……....9
Figure 2.3: The Coordinate system used for brachytherapy dosimetry calculations 13
Figure 3.1: (a) A photograph showing the applicators that were used for this study. (b) A graphical definition of the angle of the ring and IU applicator. In this study the ring angle was 60^0, i.e. the IU is 60^0 from the vertical (antero-posterior) axis.....19
Figure 3.2: The CAD drawing showing the positions of the RPLGDs in the plane of the IU in the phantom when the ring and 6 cm IU in place.....20
Figure 3.3: The CAD drawing showing ring and 6 cm IU for the top view.....21
Figure 3.4: The CAD drawing of the phantom with the ovoids and IU of 6 cm showing the top view on a scale of 10:1.....21
Figure 3.5: The CAD drawing for the phantom with the ovoids and IU front view on a scale of 10:1. 22
Figure 3.6: The phantom with Joslin Flynn applicator set in place. Two RPLGDs are also shown positioned on either side of the IU in the plane of Point A and B 23
Figure 3.7: The phantom with the 60^0 ring and 6 cm IU applicators positioned in the water phantom. 24
Figure 3.8: The Dose Ace RPLGD reader.....25
Figure 3.9: Schematic of RLPGD. On the left hand side (marked “123” in the figure) is the serial number and the readout area is on the opposite end, 0,6 mm in length. The diameter of the incident laser beam is 1mm (Hsu, 2006). 26
Figure 3.10: The 20 mm sorbo treatment plan showing the coronal view on a scale of 1:1. 29
Figure 3.11: The axial view of the dose distribution around the 26 mm diameter ring and 6 cm IU. The geometric position of point A is indicated with a sky blue cross. 29
Figure 3.12: The planning of 26-ring and 6 cm IU tube applicator. The geometric point A is indicated with a sky-blue cross. 30

Figure 3.13: : The plan delivery to ring and 6 cm IU tube applicator where glass dosimeters are 2 cm from the centre of the IU tube applicator. 31
Figure 3.14: The plan delivery to ovoid's and 6 cm IU tube applicator where glass dosimeters are 2 cm from the centre of the IU tube applicator. 31
Figure 3.15: The sagittal view of brachytherapy applicators in the phantom as modelled by MCNP code. 33
Figure 3.16: (a) Geometric design of the GammaMed HDR 192Ir source (Reyes-Revera et al,. 2014). (b) MCNP source model 34
Figure 4.1: The image shows the isodose lines passing through the glass dosimeter, the blue isodose line representing 8 Gy. Orange and green is are 9 Gy and 6.50 Gy respectively. 36
Figure 4.2: The sensitivity correction factors for 20RPLGD. 38
Figure 4.3: The graph of glass dosimeter signal reproducibility presented as percentage standard deviation for 20 glass dosimeters. 40
Figure 4.4: The linearity in the response of the RPLGDs with dose up to 3.5 Gy 41
Figure 4.5: Comparison of the doses calculated by the TPS to those measured by the RPLGDs around a 20mm sorbo applicator. 43
Figure 4.6: Comparison of the dose calculated by the TPS to those measured by the RPLGDs for 26 ring tube and 6 cm IU applicator 44
Figure 4.7: Comparison of doses calculated by the TPS to those measured by the RPLGDs for ovoids tube and 6 cm IU tube applicator 45
Figure 4.8: The image shows the MC doses for ring and 6 cm IU tube applicator 46
Figure 4.9: The 2-dimensional view of the dose distribution modelled by MCNP code normalised at 20 mm radial distance from the centre of the applicator 47
Figure 4.10: Comparison of doses calculated by the TPS and (MC) to those measured by the RPLGDs for 26 ring tube and 6cm IU applicator 48
Figure 4.11: Comparison of the doses calculated by the TPS and (MC) to those measured by the RPLGDs for Ovoids tube and 6cm IU applicator. 49

List of Tables

Table 4.1: The summary of 60 RLPGDT's sensitivity correction factors and percentage standard deviations 37

Table 4.2: The reproducibility percentage standard deviations of 60 RPLGDs 39

Table 4.3: The linearity response and percentage standard deviations for 45 RPLGD's 41

Table 4.4: The RPLGDs calibration factor for Co-60 Teletherapy machine 42

Table 4.5: The RPLGDs done verification at 4 positions in the water phantom 43

Table 4.6: Comparison of doses calculated by the TPS to those measured by RPLGDs for 26 ring and 6cm IUapplicator 44

Table 4.7: Comparison of doses calculated by the TPS to those measured by RPLGDs for Ovoids and 6cm IU applicator 45

Table 4.8: The dose calculated by TPS and MC for R26 and IU of 6cm tube showing the left and right-side applicator 46

Table 4.9: The dose calculated by TPS and MC for Ovoids and IU of 6cm tube showing the left and right-side applicator 47

Table 4.10: The Comparison of measured and calculated doses at different distances from point A for the 26 cm diameter ring and 6 cm IU 48

Table 4.11: The Comparison of measured and calculated doses for ovoids and 6 cm IU 49

Table 4.12: The uncertainty budget for the experimental determination of the agreement between TPS planned and designed phantom glass dosimeter dose 51

CHAPTER ONE

INTRODUCTION

South African Medical Physicists have voluntarily participated in IAEA/WHO postal audits of radiotherapy high energy photon beam dosimetry for more than 2 decades. Radiotherapy utilises ionising radiation to treat cancers, and sometimes a combination of modalities is used: such as external beam radiotherapy and brachytherapy, depending on a number of factors, including the tumour site and extent. Brachytherapy is a form of treatment using small radioactive sources transferred within or very close to the tumour. The high dose is delivered to the tumour with rapid fall-off, enabling the sparing of surrounding normal structures.

Therefore, this technique requires a high standard of precision in source positioning to achieve accurate dose delivery to the target. HDR brachytherapy after-loading systems are developed in such a way to enable radioactive sources to be transferred directly from a shielded storage container into the applicators remotely. The system uses a driving mechanism to move the source to programmed channel positions using a timer control system.

Brachytherapy techniques are divided into low dose rate (LDR) treatment, whereby the radioactive materials are implanted in the tumour and deliver a dose rate in the range of 0.4 to 2 Gy per hour; medium dose rate (MDR) which delivers 2 to 12 Gy/hr; and high dose rate (HDR), which delivers dose rates over 12 Gy per hour. Pulsed dose rate (PDR) brachytherapy utilises sources and equipment similar to HDR but the dose is delivered in pulses, for example, 10 to 15 minutes every hour with repeated lower dose pulses to simulate a low dose rate approach (Gerbaulet et al. 2002).

1.1. Dosimetry audits

Radiotherapy dosimetry audits are now obligated by law in some European countries as an important part of a quality management system (Palmer et al. 2014). The Group European Curietherapy – European Society for Radiotherapy Oncology Brachytherapy Physics Quality System (GEC-ESTRO BRAPHYQS) network has developed an audit methodology for brachytherapy using the Baltas phantom to validate geometric reconstruction for applicators based on the EQUAL (ESTRO quality assurance network) – ESTRO mailing system (Palmer et al. 2014). The International Atomic Energy Agency (IAEA) / World Health Organisation (WHO) coordinates the largest dosimetric audit network for reference dosimetry of high energy photon beams at present (Palmer et al. 2014). There are also national audit groups, such as the Institute of Physics and Engineering in Medicine (IPEM), which coordinates audits in the United Kingdom (UK) via a number of regional groups (Palmer et al. 2014).

Auditing allows an independent check to be made of specific components of a clinical technique, such as dose delivery or treatment-planning system procedures. Brachytherapy treatment is a common procedure in Charlotte Maxeke Johannesburg Academic Hospital (CMJAH), but currently no national dosimetry audit of brachytherapy is available. The project seeks to develop an audits methodology for brachytherapy at CMJAH.

1.2. Research objectives

Optimisation in medical radiation exposures requires essential processes for “adequate tests of equipment performance at appropriate levels” (HSE, 2006). The medical physicist has a primary responsibility to ensure the safe use of medical radiation-emitting equipment. The purpose of this study is to develop and perform an end-to-end test for high dose rate (HDR) brachytherapy for cervical cancer, by comparing planned with delivered doses around a series of different gynaecological treatment applicators in water. This was

conducted at CMJAH, which is a centre managing a large number of cervical cancer cases, using high dose rate (HDR) brachytherapy. The specific objectives are summarised as follows:

- To improve medical physics quality aspects in HDR brachytherapy treatments at CMJAH.
- To establish the end to end dosimetry in HDR gynaecological brachytherapy at CMJAH.
- To develop a methodology for gynaecological brachytherapy audits CMJAH.

1.3. The need for national external audits in brachytherapy

Formal dosimetric audits of HDR facilities have not been conducted in South Africa, despite the high risks associated with these treatments. Significant systematic errors associated with brachytherapy treatment are therefore likely to be undetected unless they are observed at follow up. Brachytherapy dosimetry audits can help to ensure the safe and effective delivery of radiation doses to patients.

If a dosimetry audit is not conducted, there could be a possibility that the organs at risk and the tumour are not receiving the intended dose, which could cause harm and increase complications to the patient. Dosimetry audits are intended to improve accuracy, minimise potential errors, avoid litigation and improve patient care. The National Metrology Institute of South Africa (NMISA) is in the process of establishing national audit capabilities for radiotherapy using a radiophotoluminescence glass (RPLG) dosimetry system.

Using glass dosimeters in this study will eliminate problems experienced when using conventional radiation dosimeters. RPLG dosimeters (RPLGDs) were found to offer advantages over thermoluminescence dosimeters (TLDs), for instance, the exhibit good uniformity, have a small size and unlimited repeatable readings (Araki et al. 2004). They were also found to have small differences in individual sensitivity, and their responses can be converted to doses directly without any correction factors. The dose is determined from

a reference RPLGD built into the readout system. The effects of environmental conditions, such as humidity and temperature, have very little impact, and the dosimeter also has low fading effects (Rah et al. 2008).

1.4. Summary of the Research Project

This project was based on assuring quality in brachytherapy treatment. The main purpose was to develop and implement an end-to-end dosimetry audit methodology of high dose rate gynaecological brachytherapy at CMJAH using RPLG dosimeters as radiation detectors. The study was performed using a commercial treatment planning system (TPS) and Monte Carlo simulations. This report contains five chapters: introduction, theoretical background, materials and methodologies, results and discussions, and conclusions, including future work.

CHAPTER TWO

Literature review

2.1. Introduction

HDR brachytherapy treatment is expected to be accurate in terms of dose distribution as it contributes to the achievement of clinical tumour control with reduced healthy structure toxicity. Because of the steepness of clinical dose-effect curves, Van Dyk et al. (1993) defined a requirement for brachytherapy treatment dose delivery of 3% accuracy in doses at 0.5 cm or more from the radiation source. IAEA has recommended that a 5% dose agreement and 2 mm spatial agreement is required for brachytherapy. Achieving control of dose delivery is very difficult, particularly in brachytherapy due to very rapid dose fall off and a multitude of aspects that affect accuracy (Palmer et al. 2012b). "A quality assurance system in radiotherapy is essential to ensure treatment delivery is consistent and as intended, this will include a multitude of Quality Control (QC) tests designed to evaluate actual operating performance in comparison to goal values, and to enable rectification/reconciliation of any differences, and a comprehensive, robust QC system should include complementary, independent external audit." (Palmer et al. 2012b).

Many errors have been reported in brachytherapy, so to detect errors there is a need to audit and improve quality. A well chamber calibration error (Dempsey 2011), confusion over units (USNRC 2009), media reports of at least two incidents involving incorrect dwell position in treatment applicators (ASAHI SHIMBUN 2013, Sydney Morning Herald 2003 and 2003b) and manufacturer safety notifications, including potentially incorrect HDR source dwell times under special circumstances, also form part of the common errors in brachytherapy (Dempsey 2011),.

An article by Ruth Pollard in The Independent Review of 12 September 2003 entitled, "Critically ill patients receive wrong radiation therapy due to human errors", said "human error was to be blamed for radiation therapy being delivered to the wrong spot in nine critically ill patients at the Prince of Wales Hospital". A computer or a treatment-planning system calculation error led to a "geographical miss" to the target site was discovered several weeks later. The Hospital Director of Medicine, John Dwyer, said that "the brachytherapy treatment was being delivered via a flexible catheter to ease the suffering of patients who were close to death". He said, "It does not appear that we did as much harm as was potentially possible, and I don't believe any patient suffered because of our mistake. However, we recognise that it was good luck, not good management". The error was described as a major system failure; the hospital implemented a revised protocol that would ensure the treatment computer was reprogrammed for each procedure.

Another case, reported by Asahi Shimbun on the 26 of December 2013, claimed that "errors were found in cases involving brachytherapy, a procedure in which a radioactive source is placed into or adjacent to the area requiring treatment." The wrong organ was mistakenly treated. The radioactive sources were placed about three centimetres from the area that they were intended to target. The hospital said the errors were caused by a problem with the medical device used in the procedure. On 17 March 2014, an urgent field safety notice about mispositioning of the source was issued by the supplier. It said, when the source was driven to the first dwell position, the cable experienced a snaking effect. Therefore, dwell positions deviated from the planned position by a difference of 2-3 mm in the direction of the applicator tip.

External audits help to check compliance with protocols so that the correct doses could be given to the patient. End-to-end testing includes the entire preparation and delivery process, with a quantitative measurement that can be evaluated at the end of the test to confirm accurate delivery of the planned treatment.

2.2. Radio-photoluminescence glass dosimeters (RPLGDs)

Radiation produces luminescence, ionisation and scintillation, and these phenomena are detected after RPLGDs are exposed to radiation. The response gives an idea of the type of radiation and its intensity. In 1949, Wely, Schulman, Ginther, and Evans manufactured the first RPLGD system (Yokota et al. 1971). Schulman applied this system in radiation dose measurements in 1951 (Yasuda et al. 1951). Schulman used luminescent material that contained a glass compound of 25% KPO_3, 25% Ba $(PO_3)_2$ and 50% Al $(PO_3)_2$, with $AgPO_3$ to form silver activated phosphate glass (Yokota et al. 1971). It was very difficult at that time to measure doses under 1 mGy with Schulman's RPLGD system because it had a high residual dose from the phosphorescence emitted from the RPLGD without any irradiation or excitation process.

The pre-mature luminescence-measuring technique and the poor quality of the excitation source for the colour centre resulted in poor measurement accuracy. However, Asahi Techno Glass Corporation (ATGC) in Japan and Karlsruhe Nuclear Research Centre (KNRC) in Germany continued to investigate RPLGDs and the readout systems, and a new RPLGD system was manufactured in 1990 (Piesch et al. 1990).

The excitation source was changed from ultraviolet into a pulsed ultraviolet laser, and the improvements in the glass material and in the readout system made the RPLGD capable of measurements of lower doses (of the order of 10 μGy) with excellent accuracy (ATG, Corporation Chiyada Techno). Based on the preliminary report by Hsu et al. on the study of the characteristics of RPLGD in radiation measurement, the radiation detection characteristics investigation of RPLGD were found to be superior to that of TLD (Hsu) since it has the re-readable capabilities. The work on the radiation measurements with self-manufactured RPLGD by Schulman in 1951 opened the history of RPLGDG applications in dose measurement (Yasuda, Troncalli). After exposure to radiation, stable colour centres are formed in the glass and more colour centres are formed with increasing radiation intensity. After irradiation with ultraviolet light, colour centres are excited and emit 600-

nm to 700-nm visible orange light, and the amount of orange light emitted from RPLGD was found to be linearly proportional to the radiation received by glass dosimeters.

The $AgPO_4$ in silver activated phosphate glass of FD-7 can be viewed as Ag^+ and PO_4^- When the tetrahedron of PO_4^- is exposed to the radiation, it loses one electron and forms a "positron hole". The electron released from the PO_4^- will combine with Ag^+ to form an Ag^0. Similarly, hPO_4 (hole formed after PO_4^- loses one electron), will recombine with Ag^+ and then gains a "positron hole" to become Ag^{2+}. Both Ag^0 and Ag^{2+} can form colour centers as shown in figure 2.1. (Hsu, 2016)

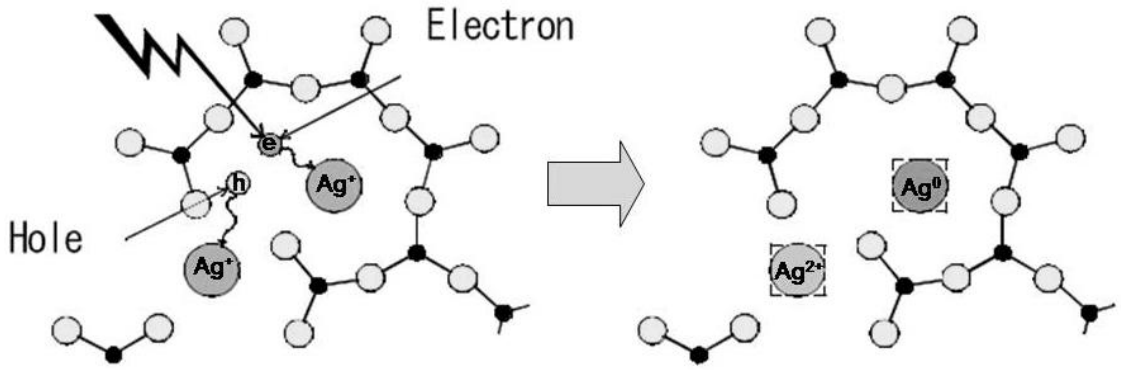


Figure 2.1. The colour centers showing motion mechanism.

After exposure, the Ag^+ in the valence band of silver activated phosphate glass combines with electrons released from both PO_4^- and hPO_4 (formed by PO_4^-) to produce colour centers (Ag^0 and Ag^{2+}). When these colour centers are excited by a 337.1nm pulse of ultraviolet laser, the electrons in Ag^0 and Ag^{2+} are excited to higher energy levels and emit 600-700nm visible orange light. **Figure 2.2** shows the energy levels of RPLGD (Hsu, 2016)

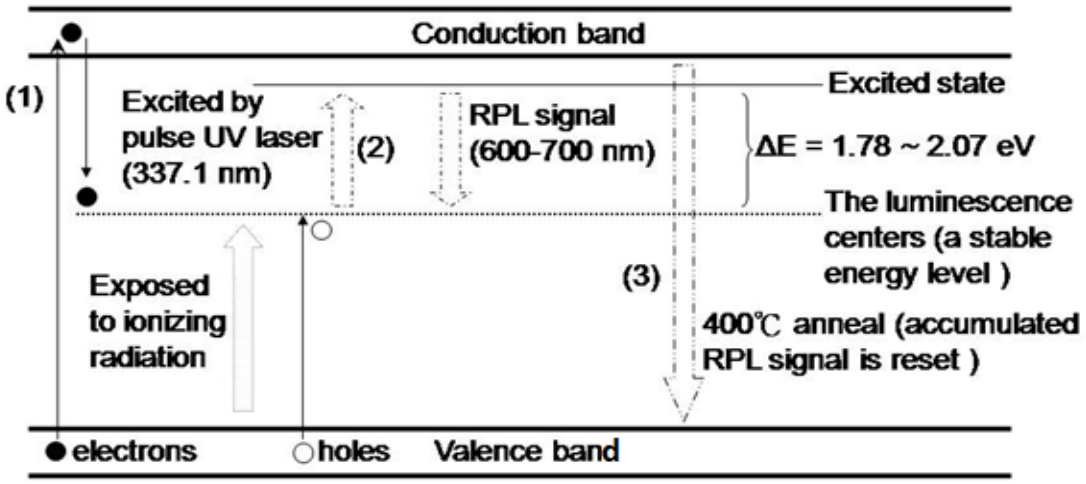


Figure 2.2. The energy levels of RPLGD. (1) After RPLGD is exposed, Ag^+ at the valence band combines with electron released from PO_4^- and hPO_4 formed by PO_4^-, to become a colour center. (2) After an electron at a colour center is excited by a 337.1 nm pulse ultra- violet laser, it will be excited and emits 600-700 nm visible orange light, before reverting to the original colour centers. (3) After annealing at 400^0C for one hour, the electron at colour centers returns to the valence band of luminescence material. (Hsu, 2016)

2.3. Characteristics of RPLGDs

RPLGDs exhibit repeatable readout; the luminescence signal does not disappear and therefore, a repeated readout for a single exposure is possible. A small difference in individual sensitivity; the readout variation between different RPLGDs with the same exposure is small. RPLGDs are manufactured with melted glass; therefore, individual sensitivity is small as compared to that of either TLD or OSLD.

The radiation exposure can be determined with the help of a readout from the reference RPLGD built-in to the readout system. Energy dependence can be reduced with an energy compensator filter hence it has small energy dependence. Small fading effects owing to the stability of colour centres in RPLGD, are exhibited. Hence, the effects of environmental conditions, such as humidity and temperature, have very little impact on colour centres, hence low fading effects for RPLGD. Better reproducibility by using pulse ultra-violet laser as an excited source, the accuracy of repeated readouts can be maintained. Therefore,

RPLGD has very good reproducibility. Wide measurable dose range: the dose linearity range for RPLGD is 0 – 500 Gy. This range covers the dose range used in the medical field.

RPLGD can therefore be applied for dose verification in radiotherapy, as well as in diagnostic radiology. RPLGD is also suitable for high dose gradient volumes, such as is found in IMRT (Intensity Modulated Radiotherapy) procedures or High Dose Rate Remote After-Loader procedures because of its small effective readout area. Feasibility of personal dose monitoring characteristics (physical and chemical) of RPLGDs are equal to or better than that of TLD and OSLD because of the luminescent material that could be read over a wide dose range and readout technique. Hence, RPLGD can also be used in occupational dosimetry.

RPLGDs are characterised as passive dosimeters when used for dose verification. The dosimeters used in this study were 1.5 mm in diameter and 8.5 mm long with an effective (or average) atomic number of 12.039 which amount to the average atomic number for the compound. When the RPLGD is exposed to ionising radiation, the amount of luminescence produced was considered proportional to the radiation dose received by the dosimeter.

2.4. HDR Brachytherapy

HDR brachytherapy is most delivered by a cylindrical Ir-192 or Co-60 radioactive micro-source of a few millimetres in length and about 1 mm diameter, which is attached to a motor-driven cable of 1 to 2.5 m in length. The source position is computer programmed. The source is driven into a transfer tube that is attached to an applicator that has previously been placed into a patient.

The source dwells at a predefined position in a particular channel for a predefined time as programmed, and then progresses to the next planned dwell position. This process is repeated to create the required dose distribution with a number of dwell positions. By varying the position and dwell time of the radiation source, the cumulative dose distribution

is made to conform to the shape of the target and avoid organs at risk. The HDR equipment is termed an *after-loader* because the applicators are positioned and imaged prior to treatment delivery.

Treatment duration is typically 5 to 20 minutes, with treatment usually fractionated over more than one session. It is critical for the success of the treatment that the applicators are correctly positioned, that the applicators do not move between imaging, treatment planning and treatment, that the treatment is carefully planned and that the source dwell positions and dwell times are accurately controlled.

"For cervix cancer treatments, the dose is historically prescribed at a position termed 'Point A', which is defined as being 20 mm along the intrauterine (IU) source tube, from the level of the ring or ovoid applicator surface, and 20 mm lateral to the IU" (Viswanathan et al. 2012). While dose distributions may now be prescribed and planned using Three-dimension Dose volume Histogram (3D DVH) parameters, with patient-specific plan optimisation, the dose to Point A is still an important parameter recorded for clinical dose reporting consistency. While several systems have been devised for dose specification in the treatment of the cervix, the two most commonly used are the Manchester system and the ICRU system (Rivard et al, 2010). The Manchester system is characterised by doses to four points: A, B, bladder and rectum. However, the duration of the implant is based on the dose rate at point A. Point B is defined 3 cm laterally to point A if the central canal is not displaced. On the other hand, the ICRU system relates the dose distribution to the target volume rather than to specific points. This report presents Monte Carlo calculations of the absorbed dose at various points using the Manchester dosimetry system.

2.5. Dose distribution measurements in HDR brachytherapy

Due to the small source size in HDR brachytherapy and its proximity to the treatment volume, there is a rapid fall-off of the dose, enabling a high dose to be delivered to the tumour with sparing of surrounding normal structures (Viswanathan & Thomadsen 2012). However, this requires high accuracy and precision of the source delivery mechanisms and the dosimetry systems. Accurate confirmation of the dose distribution delivered by the treatment equipment is critical to verify, in order to ensure that the intended prescribed radiation treatment is achieved. However, the measurement of radiation dose distributions around clinical brachytherapy sources within treatment applicators is challenging.

The volume of interest contains orders of magnitude variation in dose levels, extremely steep dose gradients near the source (around 6% per mm at the edges of the target volume in typical cervix cancer treatments) and low dose rates further away (Viswanathan & Thomadsen 2012). Conventional radiotherapy dosimetry for external beam treatments often involves relatively large detectors, but, when these are used close to a brachytherapy source, inaccuracies are introduced, due to dose averaging over the active volume. For example, a 0.6 cc ionisation chamber will exhibit a non-uniformity correction of around 10% at 20 mm and 30% at 10 mm from a brachytherapy source (Majumdar et al. 2006). The RPLGD's are very small in size and give a very high resolution compared to 0.6 cc ionisation chambers.

2.5.1 Brachytherapy treatment-planning system

Most dose calculation formalisms in brachytherapy treatment-planning systems apply a parameterisation of the single source dose distribution in water, as recommended by the Task Group # 43 of the American Association of Physicists in Medicine (Rivard et al., 2004). The dose rate in water to a point at distance r and at polar angle θ from the source is illustrated in Figure 2.3.

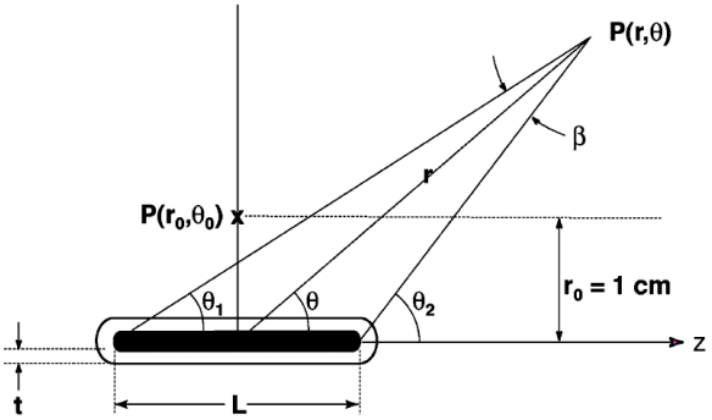


Figure 2.3. The Coordinate system used for brachytherapy dosimetry calculations.

This is expressed in eq. (2.1).

$$\dot{D}(r,\theta) = S_K \cdot \Lambda \cdot \frac{G_L(r,\theta)}{G_L(r_0,\theta_0)} \cdot g_L(r) \cdot F(r,\theta) \qquad (2.1)$$

where

$\dot{D}(r,\theta)$	is the dose rate in water at the distance r in centimetres from a line source.
θ	denotes the polar angle specifying the point-of interest
S_K	is the air kerma strength in units of cGy cm^{-1} h^{-1} U^{-1}
Λ	is the dose rate constant expressed in cGy h^{-1} U^{-1}
$G_L(r,\theta)$	is the geometry factor
$g_L(r)$	is the radial dose function
$F(r,\theta)$	is the anisotropy function

2.6. Monte Carlo technique

2.6.1 Monte Carlo simulation research in brachytherapy

Monte Carlo techniques are numerical methods employing statistical simulation. It was utilized in this study to validate the results from treatment planning system and the measured data from the brachytherapy phantom. This procedure of simulation was first established and used systematically during the Manhattan Project in the American World War II efforts to develop nuclear weapons (Harrison, 2010). With the technique named after the Monte Carlo Casino in Monaco, it was suggested by John von Neumann and Stanislaw Ulam to investigate properties of neutrons traveling through radiation shielding (X-5 Monte Carlo Team MCNP, 2003).

With the progression of time, Monte Carlo techniques have been expanded to simulate processes involving random behaviour and to quantify physical parameters that are difficult or even impossible to calculate from experimental measurements (Alireza & Mesbahi, 2010). Monte Carlo techniques have become popular in many areas of medical physics (Granero, et al., 2007), (Guerrero, et al., 2014), (Williamson & Z, 1995), because of the stochastic nature of radiation emission, transport and detection processes. To date, Monte Carlo modelling has been carried out by various simulation programs (for example, EGSnrc, MCNP, PENELOPE, and GEANT4), which in turn have been successfully applied in a variety of medical areas, such as mammography, nuclear medicine, and radiotherapy.

As in various treatment techniques in radiation therapy, Monte Carlo (MC) simulation has become a significant dosimetry tool in modern brachytherapy, playing a significant role in both clinical practice and research. The most well- known application of MC methods in brachytherapy is the determination of dose rate distributions around individual radiation

sources (Granero, et al., 2007). Experimental methods including film and thermoluminescence dosimetry in solid phantoms have been conventionally used to confirm the accuracy of treatment-planning systems (TPS) before clinical use of a TPS in brachytherapy (Alireza & Mesbahi, 2010).

The complexities of experimentally measuring single-source dose distributions caused by the sharp dose gradients, low photon energies, and dose rates associated with brachytherapy make computational dosimetry techniques, such as MC simulations an important tool in brachytherapy (Landry, et al., 2013). Although MC modelling of a 3D brachytherapy source geometry was performed as early as 1971 by (Krishnaswamy & Hale, 1971) for ^{252}Cf needles, it took another decade for the field to fully embrace 3D modelling.

The 1990s saw several studies comparing MC simulations of brachytherapy sources with thermoluminescent dosimeter (TLD) measurements (Kirov et at, 1996). These findings confirmed that the MC practice applied to brachytherapy dosimetry was sufficiently accurate enough to support clinical dosimetry. This supported the American Association of Physicists in Medicine (AAPM) Task Group No. 43 (TG-43) requirement that at least one experimental and one MC determination of dosimetry parameters be published before using a source clinically, essentially making MC simulations an industry standard (Rivard, et al., 2004). Hence, several MC studies (Granero et al, 2007) have been performed to determine the dosimetric parameters of the AAPM TG-43 for different source specifications (Eckert & Ziegler BEBIG Co0.A86, Varian Medical Systems GammaMedPlus iX, Nucletron Corporation MicroSeletron) and using different Monte Carlo codes (MCNP, BEAM, EGSnrc, PENELOPE, GEANT4, and ETRAN/ITS). A joint AAPM/ ESTRO report (Perez-Calatayud, et al., 2012) on high-energy brachytherapy dosimetry applied the AAPM prerequisite (Li, et al., 2007) to several ^{192}Ir, ^{137}Cs, and ^{60}Co source models was recently published. This increasing production of new brachytherapy sources and dosimetry datasets is associated with a rapidly growing number of MC-related brachytherapy publications in the peer-reviewed literature (MCNP5 Development team, 2005 and Yang et al, 2009).

The practice of MC methods in brachytherapy now goes beyond single-source dosimetry. An important area of current research is the application of MC simulations to perform patient-specific dose calculations. This is necessary to overcome the limitations of TG-43-style table-based source-superposition algorithms, which include neglecting interseed attenuation (ISA) and tissue heterogeneities for low-energy seed implants (Burns et al, 1989), and neglecting applicator shielding and partial scattering effects for higher-energy brachytherapy procedures (Valicenti et al, 1995). Similarly, Lemarechal et al, (2015). implemented and evaluated an accurate and fast Monte Carlo Simulation (MSC) on Graphics Processing Units (GPU) for brachytherapy low dose rate (LDR) applications. This technique was compared to the current clinical standard (TG43) dose calculation formalism.

2.6.2 MCNP code

MCNP is a general-purpose Monte Carlo N–Particle code that can be used for neutron, photon, electron, or coupled neutron/photon/electron transport, including the capability of calculating eigenvalues for critical systems (X-5 Monte Carlo Team MCNP, 2003). The code treats an arbitrary three-dimensional configuration of materials in geometric cells bounded by first- and second-degree surfaces and fourth-degree elliptical tori (X-5 Monte Carlo Team MCNP, 2003). The MCNP system is maintained by a large group at Los Alamos National Laboratory and has many applications outside medical physics because it was originally a neutron–photon transport code used for reactor calculations. An overview of principles governing the operation of MC codes has been provided in (X-5 Monte Carlo Team MCNP, 2003). In addition to the code capabilities of MCNP5, MCNP6 includes several significant new capabilities such as adjoint based sensitivity coefficients, geometry mesh file creation, unstructured mesh geometry, and low energy photon and electrons, and many more.

The implementation of the code requires the user to generate an input file that contains information about the problem that includes geometry specification, description of materials and selection of cross-section evaluations, location and characteristics of the

radiation source, i.e., neutron, photon, or electron, the type of answers or tallies desired, and any variance reduction techniques used to improve efficiency (X-5 Monte Carlo Team MCNP, 2003).

CHAPTER THREE

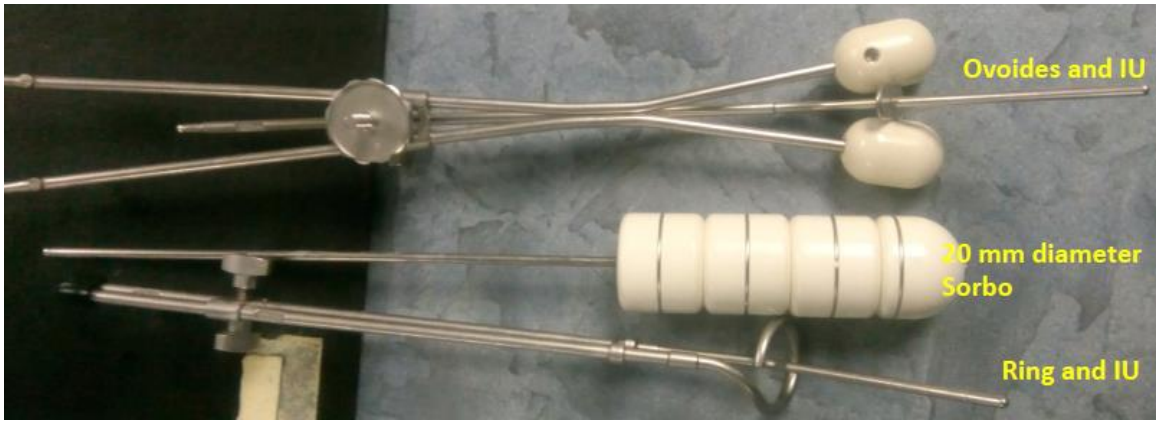
Materials and Methodology

3.1. Introduction

The objective of this research was to verify the correct delivery of the treatment plans used for gynaecological brachytherapy applications in accordance with the CMJAH protocols. Different techniques were employed that included computed doses from the treatment plans, RPLGD measurements and Monte Carlo simulations.

3.2. Equipment and materials

A water phantom was designed using CAD (Computer Aided Design) software to perform Ir-192 HDR brachytherapy absolute-dose measurements in the water around an applicator using a fixed geometry. The calibrated Standard Imaging brachytherapy 90008 well chamber was utilised to confirm the reference air kerma rate of the source and a Cs-137 check source was used for chamber stability. Dose Ace Xe RPLGDs and a reader Model FGD-1500 was used. A General Electric computed tomography (GE-CT) scanner, Varian GammaMed Plus iX HDR remote after loading unit, and a 3D BrachyVision planning system version 13 were used. A rigid ring applicator with a diameter of 26 mm connected to an intrauterine (IU) applicator of 6 cm long was used. The IU and ring applicator set of 60^{o} was used. In addition, a 20 mm diameter sorbo of length 8 cm was also studied, as well as a Joslin Flynn ovoid applicator with an IU of 6 cm. The applicators are shown in Figure 3.1 (a) and a diagram showing the configuration of the 60^{0} ring and IU set is shown in Figure 3.1 (b). A cobalt-60 (Theratronics Equinox) unit was used to calibrate the RPLGDs. All equipment used for this research project was available at the CMJAH or NMISA.



(a)

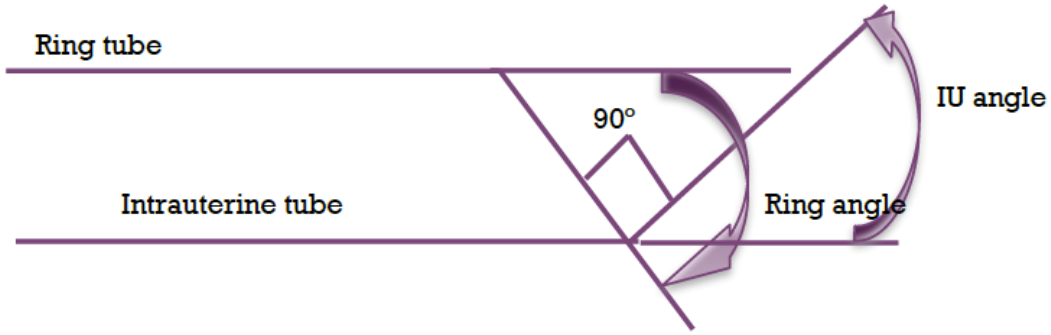


Figure 3.1: (a) A photograph showing the applicators that were used for this study. (b) A graphical definition of the angle of the ring and IU applicator. In this study the ring angle was 60^0, i.e. the IU is 60^0 from the vertical (antero-posterior) axis.

3.3. Method

To develop a brachytherapy dosimetry audit methodology, the standard operational procedures at CMJAH were followed. However, a phantom was utilised instead of a patient, and the local clinical treatment protocol at CMJAH was followed in terms of the applicator type, prescription level, dose and source dwell positions (template) or plan library normally selected according to the disease extent for a particular individual patient.

3.3.1. Phantom design

CAD software version 18 was used in order to design a water phantom to accommodate an applicator such that RPLGDs could be positioned accurately at point "A. Additional RPLGDs were placed parallel to the dosimeter at point "A" at 1 cm intervals up to 7 cm laterally as shown in **figure 3.2, 3.3, 3.4, 3.5 and 3.6** according to different applicators used. The phantom was designed in such a way that it accommodated all the applicators that were used in this study.

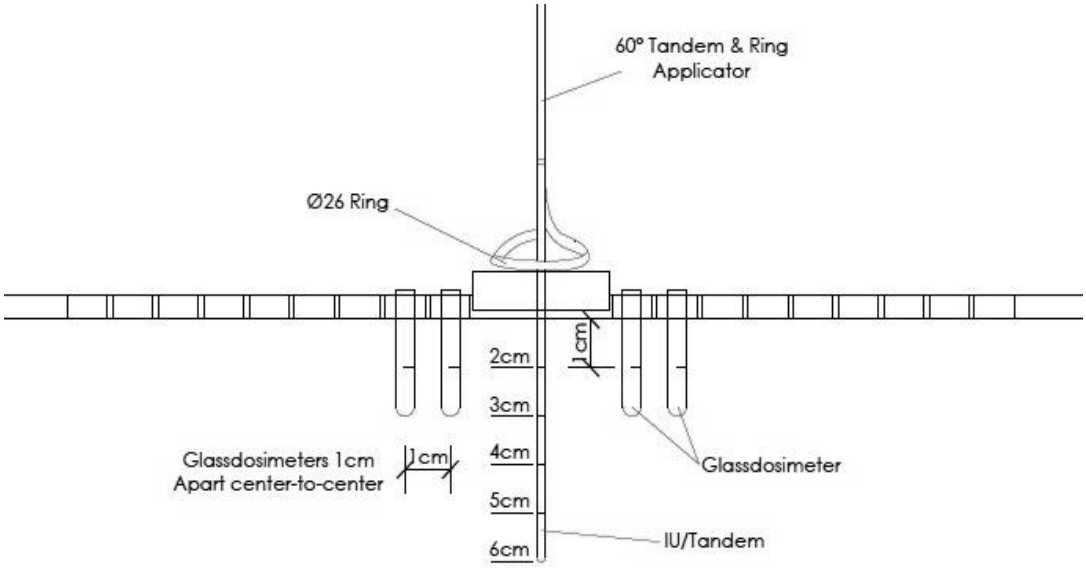


Figure: 3.2 The CAD drawing showing the positions of the RPLGDs in the plane of the IU in the phantom with the ring and 6 cm IU in place.

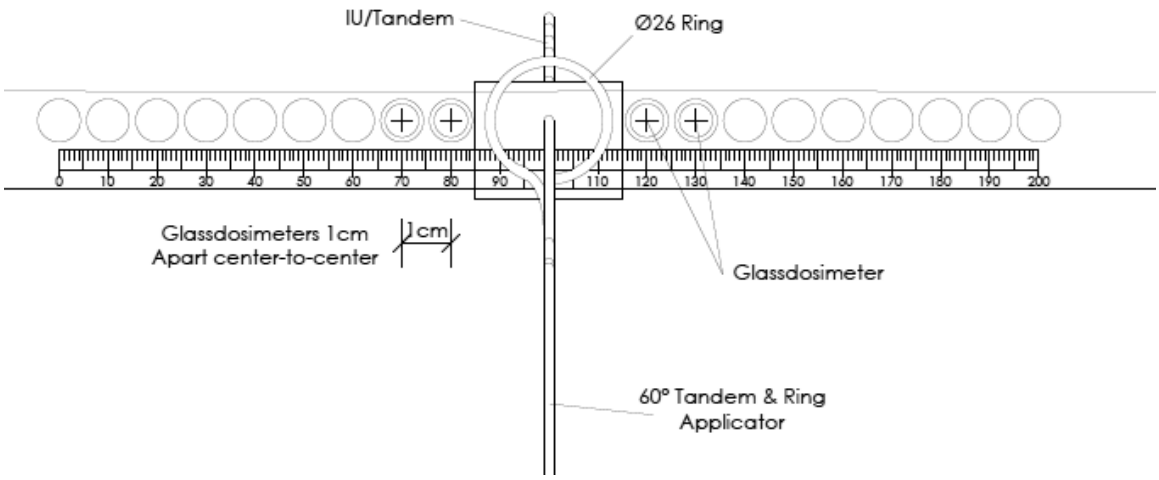


Figure 3.3: The CAD drawing showing ring and 6 cm IU for the top view.

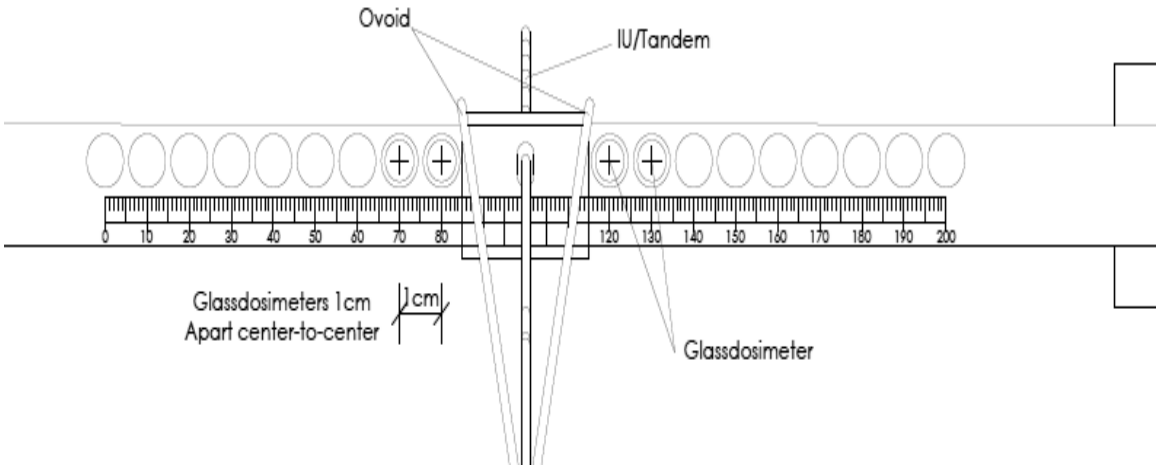


Figure 3.4: The CAD drawing of the phantom with the ovoids and IU of 6 cm showing the top view on a scale of 10:1.

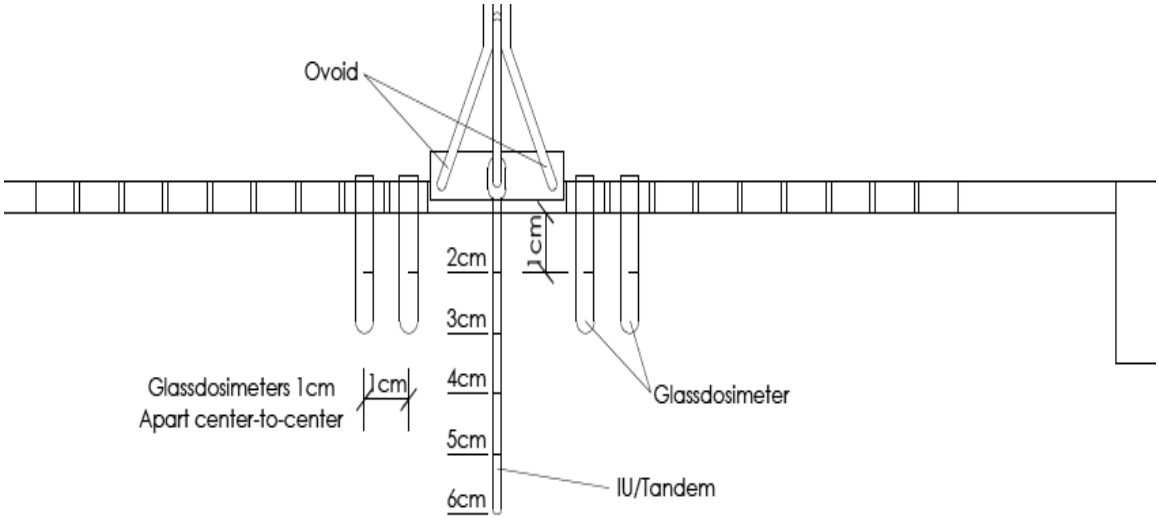


Figure 3.5 : The CAD drawing for the phantom with the ovoids and IU front view on a scale of 10:1.

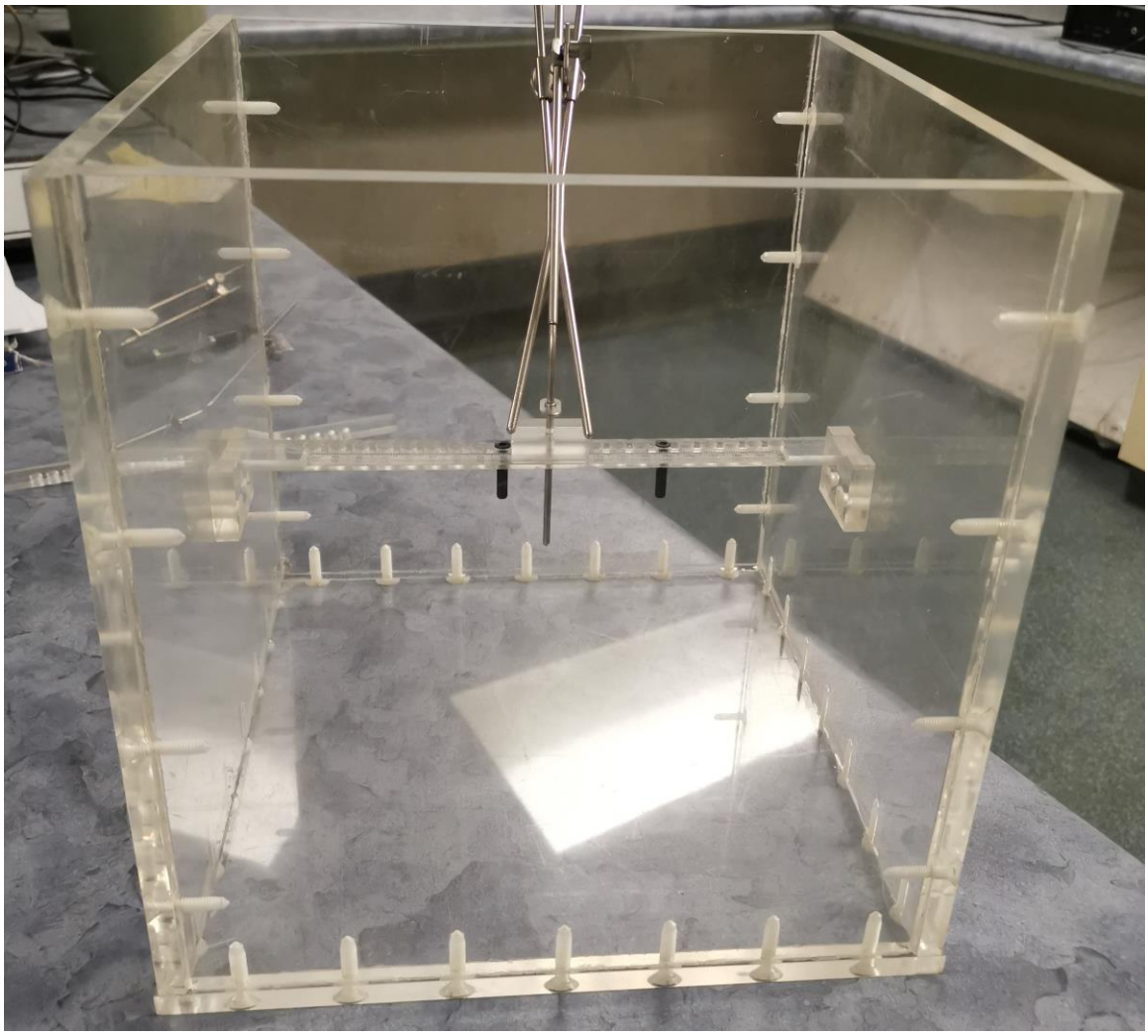


Figure 3.6: The phantom with Joslin Flynn applicator set in place. Two RPLGDs are also shown positioned on either side of the IU in the plane of Point A and B

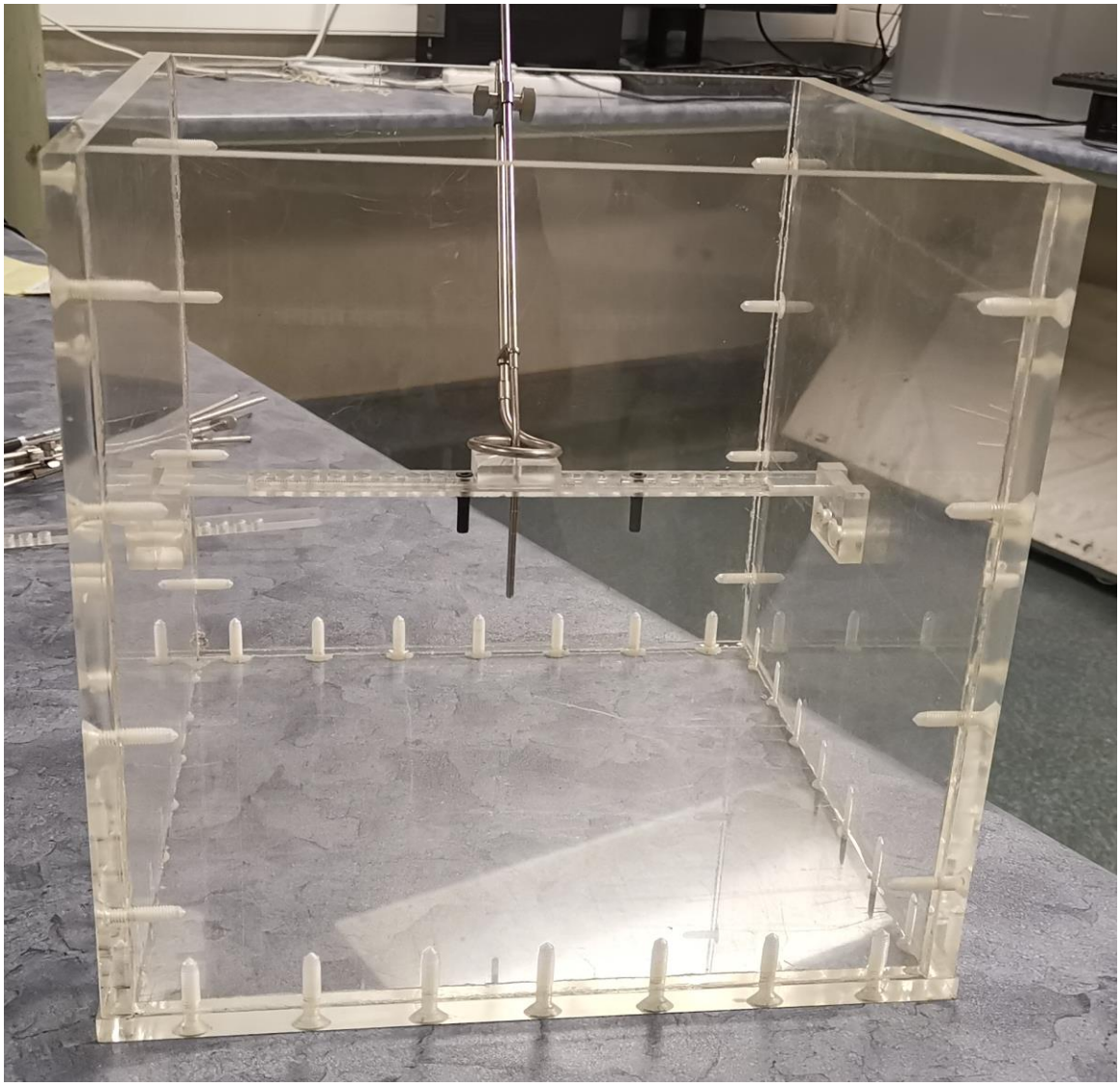


Figure 3.7: The phantom with the 60^0 ring and 6 cm IU applicators positioned in the water phantom.

In this work, the absolute dose was verified at different points for a treatment plan generated to deliver a Manchester-based treatment technique. The phantom had a perspex insert placed across the inner volume to allow the positioning of glass dosimeters at the coordinates corresponding to Manchester A and B points, as well as five sets of additional points which were positioned at 1 cm intervals in the same lateral plane as that of the Manchester A and B points so that the resulted values will be compared with planning system and MCNP results. The same insert also allowed for the fixation of a ring and tandem or a tandem and ovoids applicators in typical gynaecological treatment geometry.

3.3.2. RPLGD preparation

The pulsed Ultraviolet (UV) laser excitation method was used for the readout of the RPLGDs. When the glass dosimeters are exposed to ionising radiation, stable luminescent centres appear and, when excited by UV- rays, the glass emits an orange luminescence. Two hundred RPLGDs were prepared for this study and the initial annealing process was achieved by annealing at 400^{o}C for 1 hour. The magazine was removed once it had cooled to 40^{o}C. The glass elements were placed into holders for irradiation. After irradiation, the elements were preheated to 70^{o}C for 1 hour to stabilise the luminescence centres. After re-cooling to room temperature, the glass elements were taken out of the holders and the accumulated radiophotoluminescent signal was read out as the reader shown in **figure 3.8**.

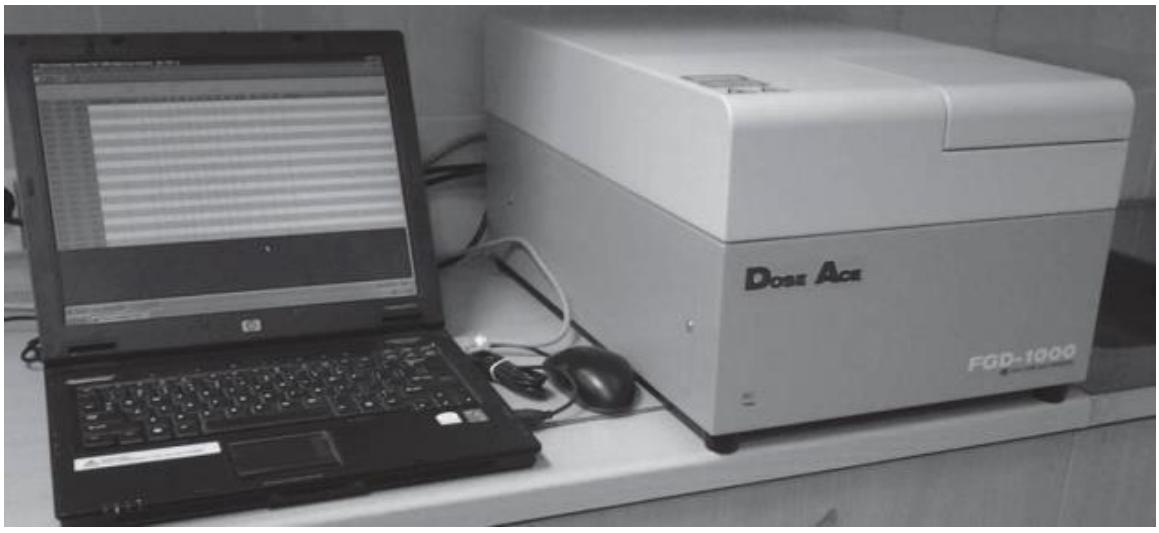


Figure 3.8: The Dose Ace RPLGD reader.

The Dose Ace reading system consisting of GD-302 M glass rods from Asahi Techno Glass Corporation was used. RPLGDs are made of silver activated phosphate glass with an ID number printed on one end and are encapsulated in black watertight capsules, with the same ID number as the rod glass inside. The Favourable Glass Dosimetry (FGD) reading system could accommodate 20 glass rods. The schematic diagram of RLPGD is shown in **figure 3.9**.

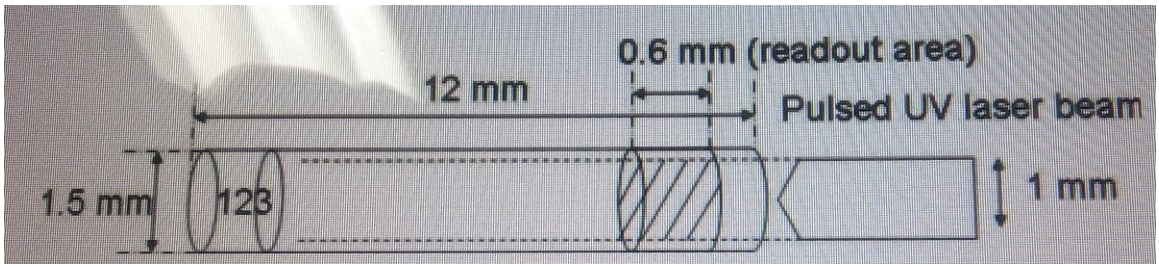


Figure 3.9: The Schematic of RLPGD. On the left-hand side (marked "123" in the figure) is the serial number and the readout area is on the opposite end, 0,6 mm in length. The diameter of the incident laser beam is 1mm (Hsu, 2006).

3.3.3. Determination of dosimeters characteristics

3.3.3.1.Glass rod dosimeter sensitivity correction factor

The RPLGD glass rods were exposed to 2 Gy in the cobalt-60 beam and the sensitivity correction factor was quantified as the ratio of the average reading of the group of dosimeters to the reading of each individual RPLGD rod glass.

3.3.3.2.Readout position correction

The glass dosimeters were placed in a tray accommodating 20 RPLGDs, and the response depended on the positions in the readout tray was observed. A number of readout trays were tested at NMISA, and those with the smallest readout position corrections were selected for use in this study. A position correction factor was unique to each tray because of small geometrical differences affecting the readout area alignment to the built-in laser system.

Following the exposure to 2 Gy, four repeat readings of each dosimeter were performed. After each reading, the positions of the RPLGDs were checked, to ensure that the glass dosimeters did not rotate. The standard deviation of the mean for four readings were calculated.

3.3.3.3. RPLG reproducibility

Since glass dosimeters can be irradiated and annealed for reuse, a test was done to monitor the stability of the sensitivity corrections. Sixty RPLGDs were exposed three times to a

dose of 2 Gy, read and annealed, and their sensitivity was recalculated after each irradiation and readout cycle. The standard deviation of the three cycles were quantified.

3.3.3.4. Dose-response non-linearity

The relation between the dose delivered and the reading measured was checked for a dose range of 0.12 - 3.5 Gy. Five glass rod dosimeters were irradiated in reference conditions in the Co-60 beam. The dose-to-signal response was normalised to the dose of 2 Gy, and a correction function for the non-linearity in the dose response was determined.

3.3.4. Glass dosimeter calibration using a cobalt teletherapy beam

A high-energy Co-60 teletherapy beam was utilised to calibrate the RPLGDs for use in brachytherapy. The absorbed dose to water is well established in the Co-60 beam and has been determined accurately with traceable standards using ionisation chambers and dosimetry protocols. The RPLGDs were irradiated in a water phantom at a depth of 5 cm at a Source to Axis Distance (SAD) of 80 cm in a 10 x 10 cm^2 field. The times were calculated to give 2 Gy at a depth of 5 cm from the surface in a water phantom. Nine glass dosimeters were exposed to the same dose of 2 Gy at the same setup. The calibration value was achieved by determining the calibration factor using equation (1).

$$\mathbf{Dose = M \times N_{RPLGD} \times f_{unif} \times f_{mag} \times f_{scf} \times f_{fad} \times f_{lin}} \quad (3.2)$$

Where;

M is the RPLGD reading

NRPLGD is the calibration factor

Funif is the beam off axis correction factor

Fmag is the magazine position correction factor

Fscf is the sensitivity correction factor.

Ffad is the fading correction factor

Flin is the dose non linearity correction factor

The glass signal to dose calibration factor (N_{RPLGD}) was calculated from the reference signal using equation (3) below.

$$\mathbf{N}_{\mathrm{RPLGD}} = \frac{\mathrm{D}_{\mathrm{ref,corr}}}{\mathrm{GS}_{\mathrm{corr}}} \qquad (3.3)$$

Where $D_{ref,corr}$ is the Co-60 given dose corrected for dose non-uniformity in the phantom.

GS_{corr} is the corrected glass dosimeter signal.

3.3.5. RPLGDs position verification

A 20 mm diameter vaginal applicator was used to verify the positional accuracy of the dosimeters in the phantom. The applicator was inserted into the phantom and was CT scanned. The images were transferred to the brachytherapy planning system, and a dose of 5 Gy was prescribed at 1 cm from the surface of the 8 cm vaginal applicator in the central axial plane. The plan was transferred to the brachytherapy treatment unit. Two RPLGDs were positioned parallel to the applicator at the prescription point as shown in **Figure 3.11**. The positional accuracy was estimated from the difference in the dose received by RPLGDs.

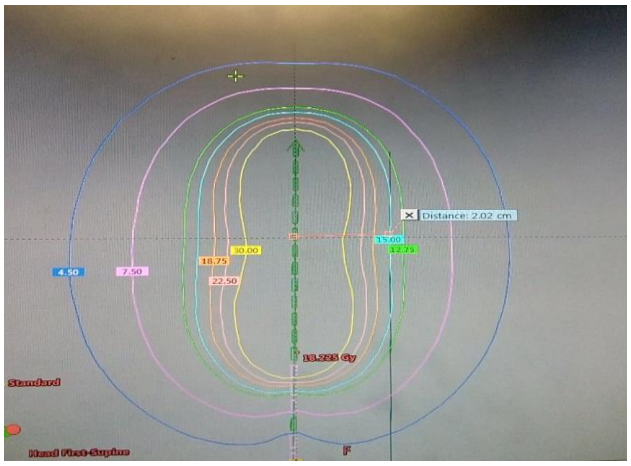


Figure 3.10: The 20 mm sorbo treatment plan showing the coronal view on a scale of 1:1.

3.3.6. CT Scan and planning

The water phantom was CT scanned with the 26 mm diameter ring and 6 cm intrauterine applicator in place. The images were exported to the brachytherapy planning system. The applicators were reconstructed from the images by windowing, also known as *grey-level mapping*, and using contrast enhancement as shown in **Figure 3.12 and 3.13**. The Ir-192 radio-activity source was 8.612 Ci on the day of measurements. Plans were created to deliver 8 Gy to point A, using a clinical protocol at CMJAH.

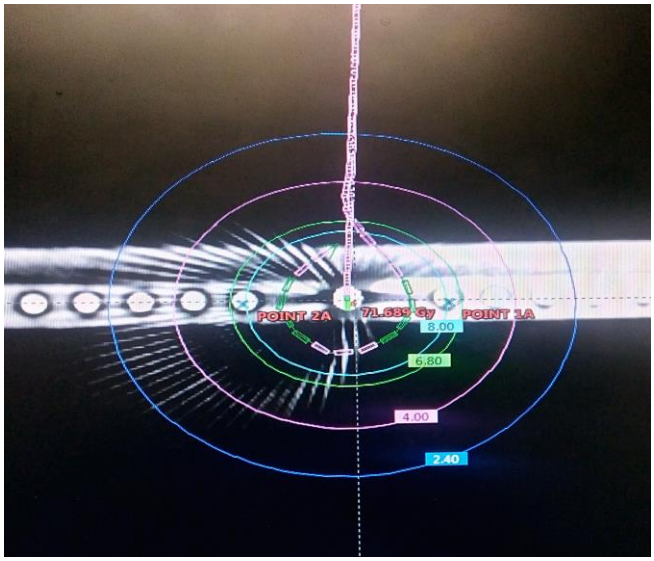


Figure 3.11: The axial view of the dose distribution around the 26 mm diameter ring and 6 cm IU. The geometric position of point A is indicated with a sky-blue cross.

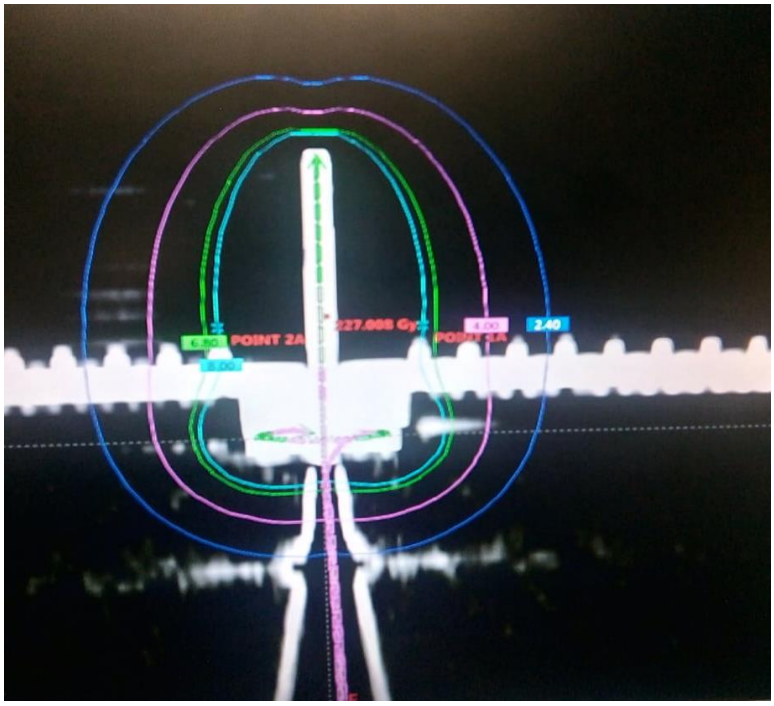


Figure 3.12: The planning of 26-ring and 6 cm IU tube applicator. The geometric point A is indicated with a sky-blue cross.

The doses calculated by the GammaMed treatment planning system from POINT "A" up to 7 cm from the centre of the IU on the left and right side, were noted.

3.3.7. Treatment delivery

RPLGDs were positioned in the phantom as shown in **Figure 3.14 and 3.15**. The planning system data were exported to the treatment unit, and the water phantom was irradiated according to the imported treatment plan. This procedure was repeated three times for each glass dosimeter position, using three different glass dosimeters. The plan was delivered for each position and the RPLGD were only position at that position. The doses calculated by the planning system were compared with results obtained from the glass dosimeters at each position.

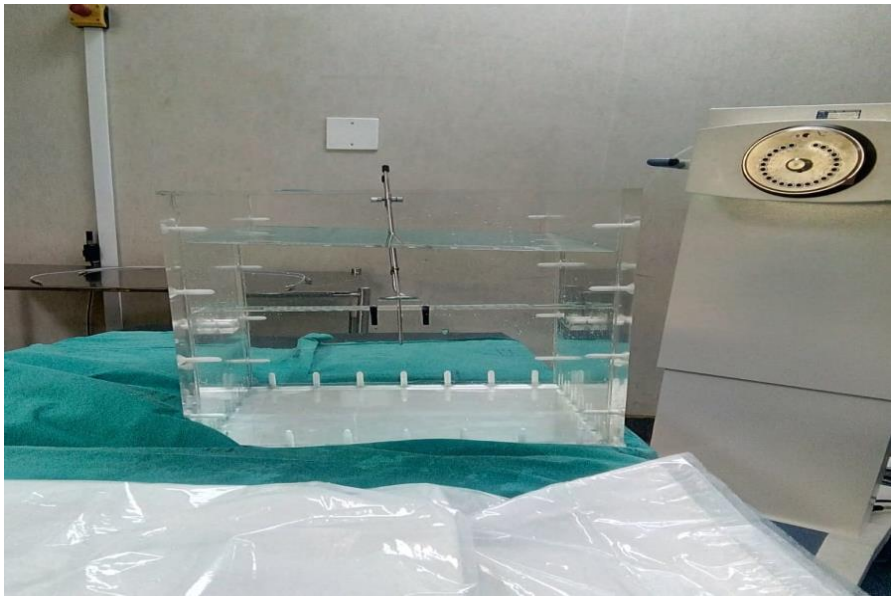


Figure 3.13: The plan delivery to ring and 6 cm IU tube applicator where glass dosimeters are 2 cm from the centre of the IU tube applicator.

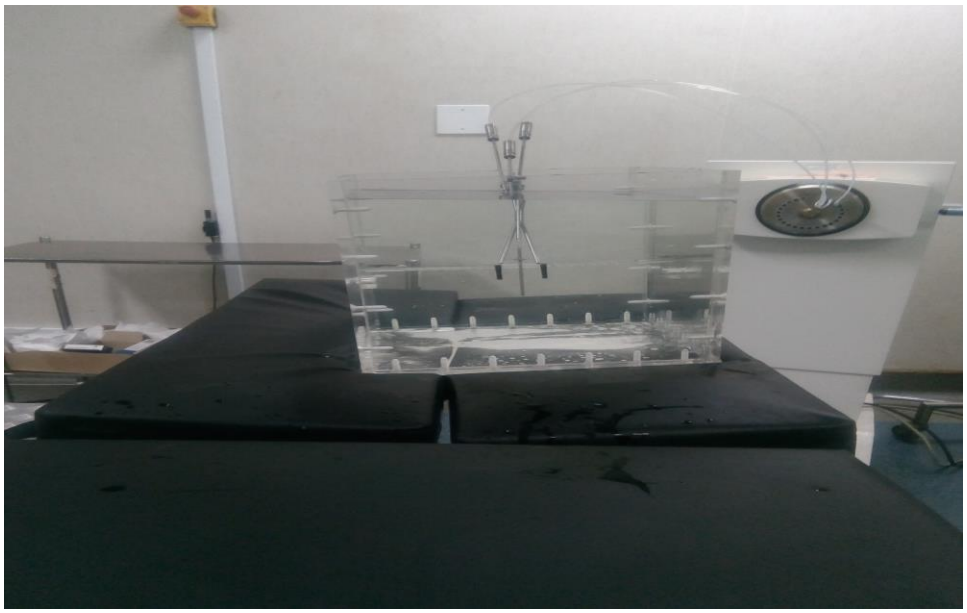


Figure 3.14 : The plan delivery to ovoid's and 6 cm IU tube applicator where glass dosimeters are 2 cm from the centre of the IU tube applicator.

3.3.8. Monte Carlo technique

It was necessary to benchmark and perform quality assurance of the Monte Carlo code for the source model to establish confidence in the reliability of simulated results. In this regard, a computational benchmarking initiative was initially performed by determining the AAPM TG-43 dosimetric parameters. This was followed by implementing the MCNP 6.1 code to simulate radiation physics principles that will result in quantifying the absorbed dose at several lateral points in the plane of point A and B for a Manchester treatment delivery system. A comparison of the results obtained was then made with those obtained from the treatment-planning system and measurements performed using RPLGD.

3.3.9. The MCNP structure

The main input file for the user contains the information to describe the problem. The structure is as shown below;

One Line Problem Title Card
Cell Cards [Block 1]
blank line delimiter
Surface Cards [Block 2]
blank line delimiter
Data Cards [Block 3]

MCNP input file has several sections given as blocks. For example, Block 1 contains cell cards that are used to define the shape and material content of the physical space of the problem. They are defined from the combination of surfaces (described in Block 2) using interceptions, unions and complement operators and surfaces are defined by supplying coefficients of surface equations recognised by the MCNP in the Cartesian coordinate system. Following the surface cards are data cards that are used to define the type of particles, problem materials, radiation sources, how results are to be scored (or tallied), the

level of detail for the physics of particle interactions, variance reduction techniques, cross-section libraries, and other user-specification cards.

3.3.10. Phantom and Source model

The simulation modelled the water phantom as illustrated in **Figure 3.16.** with the applicators fixed to the Perspex insert. Applicators were modelled following the dimensions and materials described in (Ballester, et al., 2001). The applicator's external walls were 1 mm thick stainless steel. Two applicator sets were considered. The first applicator set modelled was the ring and tandem, with four sources loaded on each side of the ring and 14 sources at 0.5 cm distance from each other along the entire 60 mm length of the IU tube, times were the standardised. The second applicator set was a combination of IU tube, which was 60 mm long, and ovoids, which were loaded with three sources on each side. In both these cases, source spacing was 0.5 cm and 8 Gy was prescribed to point A.

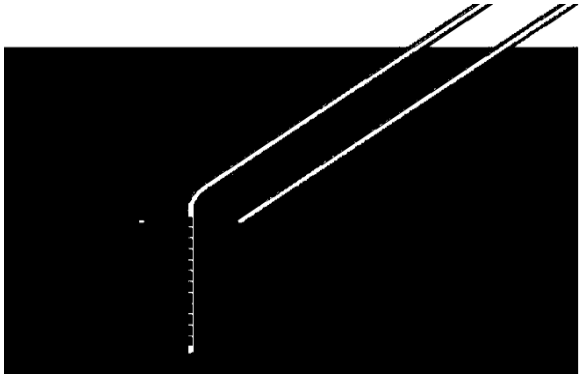


Figure 3.15: The sagittal view of brachytherapy applicators in the phantom as modelled by MCNP code.

Sources were modelled inside the applicators with source positions in the equivalent orientation to that in the treatment plan. The GammaMed Plus ^{192}Ir brachytherapy source geometric design was derived from (Ballester, et al., 2001). The active core material composition of the source comprised ^{192}Ir with an effective density of 22.42 g/cm^3. It had a 3.5 mm active length with an active diameter of 0.60 mm. The active core remained

covered by the stainless steel AISI 316L capsule of density 8.06 g/cm^3. The geometrical design and the MCNP source model are shown in **Figure 3.17.**

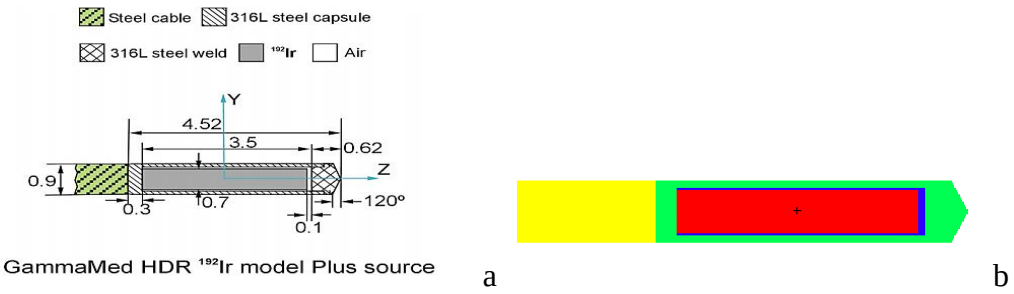


Figure 3.16: (a) Geometric design of the GammaMed HDR 192Ir source (Reyes-Revera et al,. 2014). (b) MCNP source model.

While the iridium radionuclide has both electron and gamma ray spectra, only the gamma rays' spectra were considered in the source definition card for the radioactive GammaMed Plus ^{192}Ir. This was because the contribution to the absorbed dose from electrons was negligible, due to full absorption of electrons by the stainless-steel shielding capsule (Granero, et al., 2007).

3.3.11. Monte Carlo process

The absorbed dose at Manchester points A, B points and the 5 additional points were calculated using the MCNP 6.1 Monte Carlo code. This was performed using the ^{192}Ir photon spectrum available from the (NuDat, 2008). Simulations were performed in photon and electron modes with photons and electrons being transported down to energy cut-offs of 1 keV and 5 keV respectively. Absorbed doses in the water phantom were calculated with the assumption that charged particle equilibrium existed. This assumption was considered valid if the dose contribution due to the electrons generated in the applicators were neglected.

Exactly 10^9 photons histories were run to acquire less than 1% statistical uncertainty at Manchester point B. To compute the dose at specified points, an F5 point detector tally type card was used. This tally type uses a variance reduction technique referred to as the

next event estimator. It makes a deterministic estimate of the fluence contribution at the detector point for each source particle and each collision event.

CHAPTER FOUR

RESULTS AND DISCUSSION

The test phantom was designed using CAD software to measure the dose distributions around the ring with an IU and with ovoids and IU tubes. The phantom design includes slots for the positioning of the RPLGDs. The 20 mm vaginal applicator was used to verify the position of dosimeters relative to the applicator in a well-defined geometry.

The dosimeters were exposed on a cobalt- 60 source to establish or evaluate their sensitivity, reproducibility and linearity. The GE CT scanner images were used to create treatment plans and the dosimeter position doses were measured on TPS for comparison with RPLGD doses and Monte Carlo doses. The results were analysed using a Microsoft Excel spread sheet.

The end to end testing was carried out at CMJAH and the results are summarized in **Figures 4.1 – 4.9.**

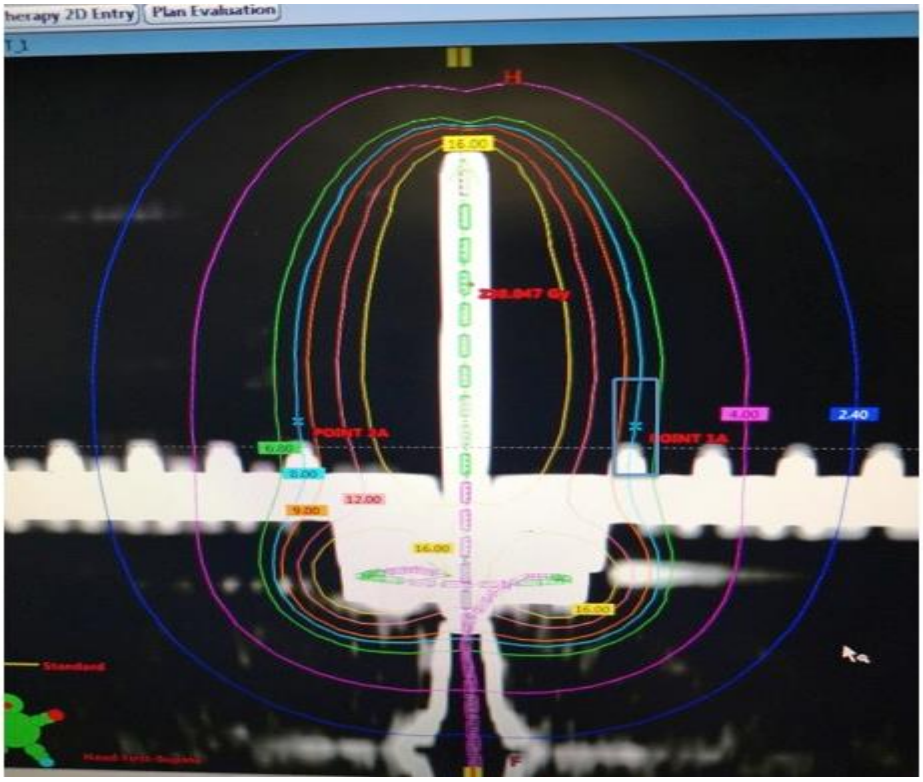


Figure 4.1: The image shows the isodose lines passing through the glass dosimeter, the blue isodose line represents 8 Gy. Orange and green are representing 9 Gy and 6.50 Gy respectively.

The blue rectangular volume drawn on figure 4.1. Shows the isodose line on the glass dosimeter which give an average of 7.9 Gy. The active readout area on the RPLGDs is located in the portion of the glass dosimeter on the opposite end from where the serial number is marked. The precise location of the active readout area is shown in **figure 3.9.**

The respond of the RPLGDs was satisfying considering that the readout area has an active length of 0.6 mm and a total active volume of less than 1 mm^3.

4.1. Sensitivity correction factor

The readout variation between different RPLGDs with the same exposure was evaluated for three different trays. The response is shown on table 4.1 and **figure 4.2**, showing the mean, standard deviation, and sensitivity correction factor.

RPLGDs	Tray 1	Tray2	Tray3	AVERAGE	%STDEV	Sensitivity correction factor
1	1928000	1925000	1927000	1926667	0.079	0.977
2	1915000	1919000	1914000	1916000	0.138	0.970
3	1957000	1955000	1953000	1955000	0.102	0.988
4	2003000	1996000	2002000	2000333	0.189	1.010
5	1986000	1988000	1984000	1986000	0.101	1.004
6	2018000	2016000	2016000	2016667	0.057	1.019
7	1954000	1955000	1948000	1952333	0.194	0.988
8	1964000	1964000	1969000	1965667	0.147	0.994
9	1967000	1961000	1956000	1961333	0.281	0.992
10	1965000	1964000	1961000	1963333	0.106	0.992
11	1944000	1948000	1943000	1945000	0.136	0.982
12	1944000	1939000	1942000	1941667	0.130	0.978
13	1969000	1973000	1970000	1970667	0.106	0.990
14	1990000	1993000	1995000	1992667	0.126	1.000
15	2002000	2012000	2009000	2007667	0.256	1.007
16	1960000	1961000	1959000	1960000	0.051	0.984
17	2016000	2013000	2017000	2015333	0.103	1.008
18	1988000	1989000	1987000	1988000	0.050	0.997
19	1997000	1993000	1995000	1995000	0.100	1.000
20	2002000	1994000	1993000	1996333	0.247	1.000

Table 4.1: The summary of 60 RLPGDs sensitivity correction factors and percentage standard deviations.

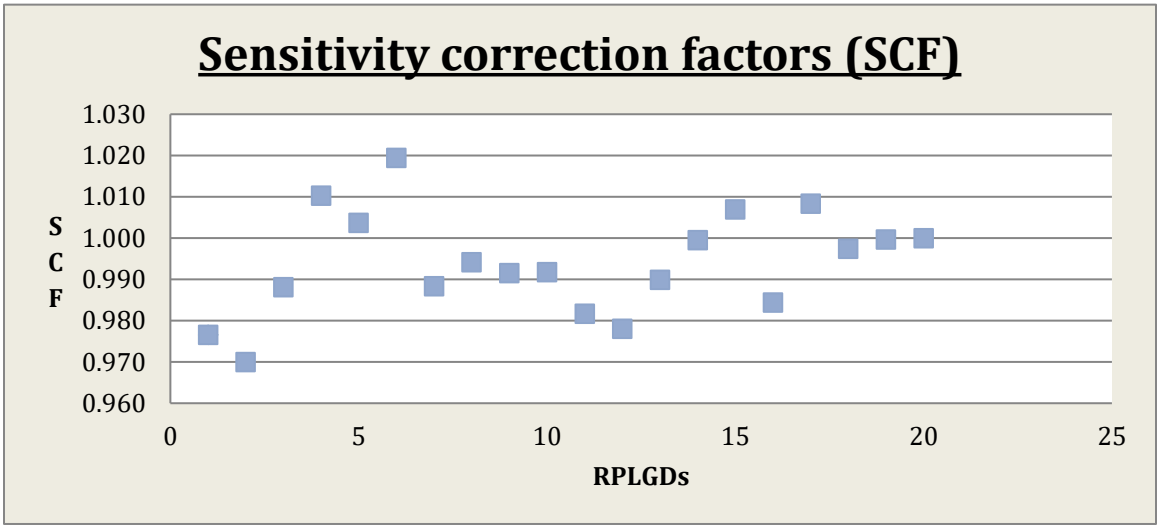


Figure 4.2: The sensitivity correction factors for 20 RPLGDs

The variation in the dosimeters' sensitivity factors was within 0.28 % for the 60 RPLGDs that were used for this study.

4.2. RPLGD reproducibility

The accuracy of repeated exposure and readout, is shown on table 4.2. and **figure 4.3.** A very good response of RLPGDs reproducibility was observed. The standard deviation of the mean of three readings, were performed.

Table 4.2: The reproducibility percentage standard deviations of 60 RLPGDs

	R1	R3	R3	AVERAGE	%STDEV
1	1961000	1962000	1960000	1961000	0.051
2	1931000	1929000	1927000	1929000	0.104
3	1959000	1954000	1954000	1955667	0.148
4	1987000	1984000	1983000	1984667	0.105
5	1926000	1928000	1927000	1927000	0.052
6	1979000	1978000	1977000	1978000	0.051
7	2070000	2068000	2068000	2068667	0.056
8	2033000	2032000	2032000	2032333	0.028
9	2013000	2007000	2007000	2009000	0.172
10	2105000	2106000	2105000	2105333	0.027
11	2038000	2030000	2032000	2033333	0.205
12	2055000	2056000	2049000	2053333	0.184
13	2059000	2064000	2061000	2061333	0.122
14	2019000	2022000	2019000	2020000	0.086
15	1995000	1997000	1995000	1995667	0.058
16	1954000	1955000	1957000	1955333	0.078
17	2051000	2054000	2050000	2051667	0.101
18	2062000	2064000	2060000	2062000	0.097
19	2056000	2057000	2057000	2056667	0.028
20	2008000	2001000	2002000	2003667	0.189

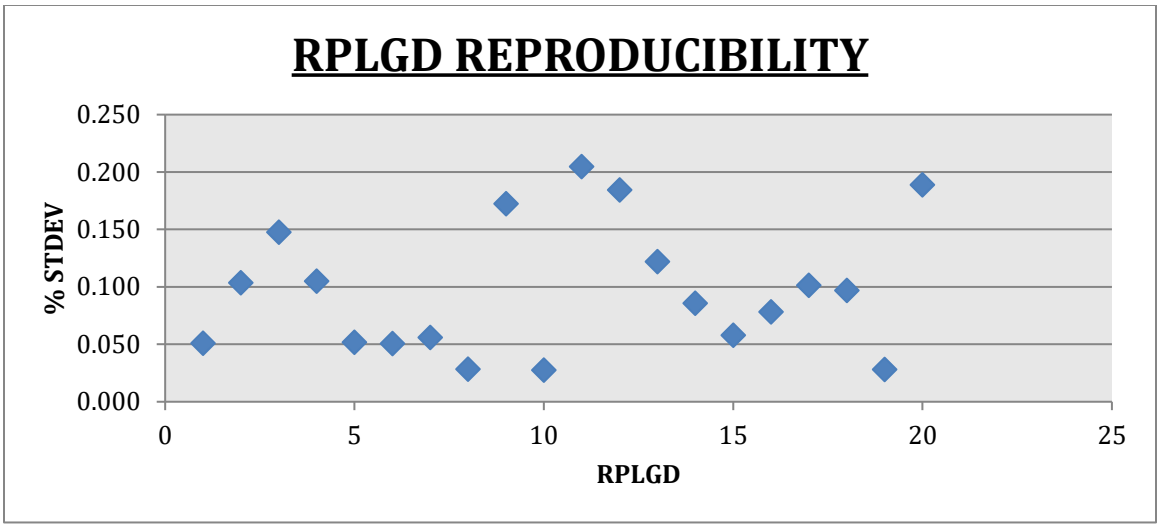


Figure 4.3: The graph of glass dosimeter signal reproducibility presented as percentage standard deviation for 20 glass dosimeters.

The reproducibility average of the standard deviation for RPLGDs measurements in this study was variating within 0.25%. which agreed well with the report from Yamashita and Arak (2004), in which they discovered the value of +/- 1.1%.

4.3. RPLGD linearity response

The dose linearity response is shown on table 4.3. The relation between the dose delivered and the signal measured was tabulated.

Table 4.3: The Linearity response and percentage standard deviations for 45 RPLGDs

	S1	S2	S3	S4	S5	AVERAGE	DOSE GIVEN (Gy)	%STDEV
1	119300	123300	124400	122600	122100	122340	0.12	1.56
2	253000	254700	257500	257200	254600	255400	0.25	0.75
3	497000	497100	500800	496700	505200	499360	0.50	0.74
4	1003000	997400	1006000	1001000	1003000	1002080	1.00	0.32
5	1488000	1481000	1520000	1519000	1517000	1505000	1.50	1.26
6	1995000	1998000	1988000	1977000	1945000	1980600	2.00	1.08
7	2436000	2420000	2445000	2421000	2395000	2423400	2.50	0.79
8	2850000	2868000	2861000	2886000	2858000	2864600	3.00	0.47
9	3345000	3372000	3395000	3388000	3352000	3370400	3.50	0.65

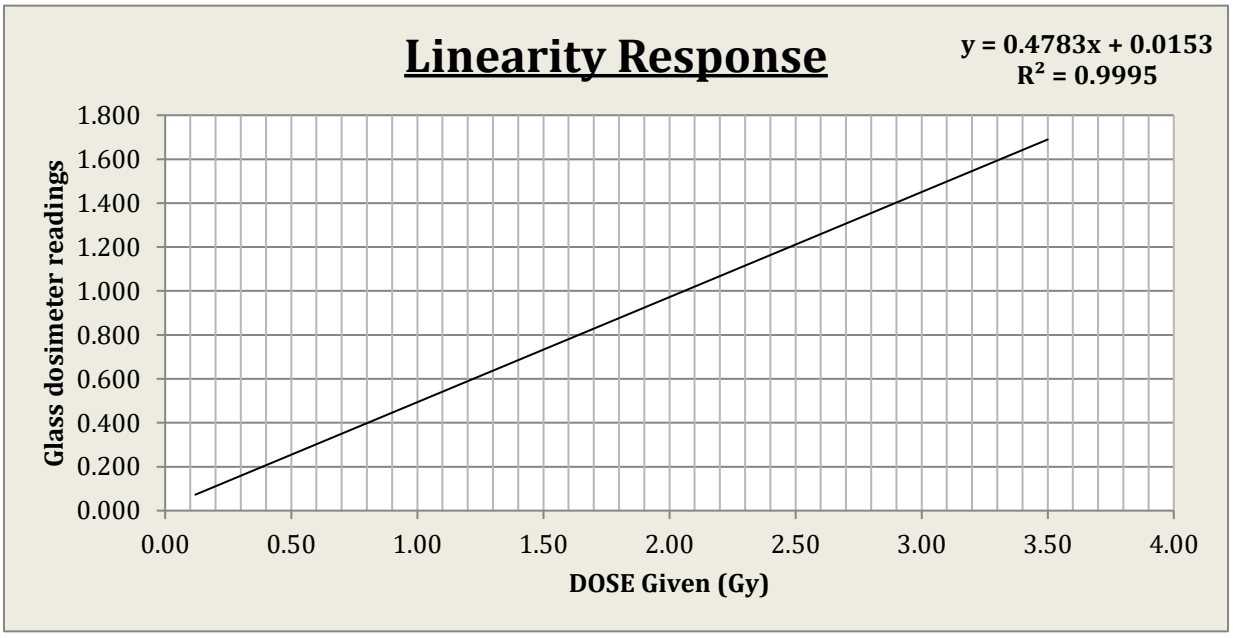


Figure 4.4: The linearity in the response of the RPLGDs with dose up to 3.5 Gy.

Linearity correction factors were obtained. The results show a variation of up to +/- 3% between doses of 0.12 Gy and 3.5 Gy on glass dosimeters. **Figure 4.4** shows the RPLGDs R^2 of 0.999. This value is in agreement with a study done by Son et at (2011), where R^2 was 0.998.

4.4. RPLGD calibration factor using a Cobalt 60 Teletherapy source

A high energy cobalt 60 teletherapy beam was utilised to calibrate the RPLGDs for use in in brachytherapy audit. Table 4.4. Provide the results of the calibration factor measured.

Table 4.4: The RPLGDs calibration factor using Co-60 Teletherapy machine

Session 1 Counts	Session 1 Counts	Session 1 Counts	Fading CF	Uniformity CF	Session Average	Given Dose (Gy)	NK_{RPLGD}
2139200	**2147200**	**2148600**	1.000	1.000	2145000	2	**9.32E-07**
2127200	**2138400**	**2126600**	1.000	1.000	2130733	2	**9.39E-07**
2128800	**2135000**	**2135600**	1.000	1.000	2133133	2	**9.38E-07**
							9.36E-07
						1/Nk	**1.07E+06**

4.5. RPLGDs position verification using 20 mm diameter sorbo

A 20 mm diameter vaginal applicator was used to verify the positional accuracy of the dosimeters in the phantom. Table 4.6 and **Figure 4.5** provides the percentage results between the TPS and RPLGD's doses.

Table 4.5: The RPLGDs dose verification at 4 positions in the water phantom

Distance from the centre of the applicator	TPS brachy dose (Gy)	RPLGD dose (Gy)	+/- % Error
2	4.92	4.92	0.02
3	3.39	3.42	1.54
4	2.49	2.47	0.81
5	2.01	1.99	0.76

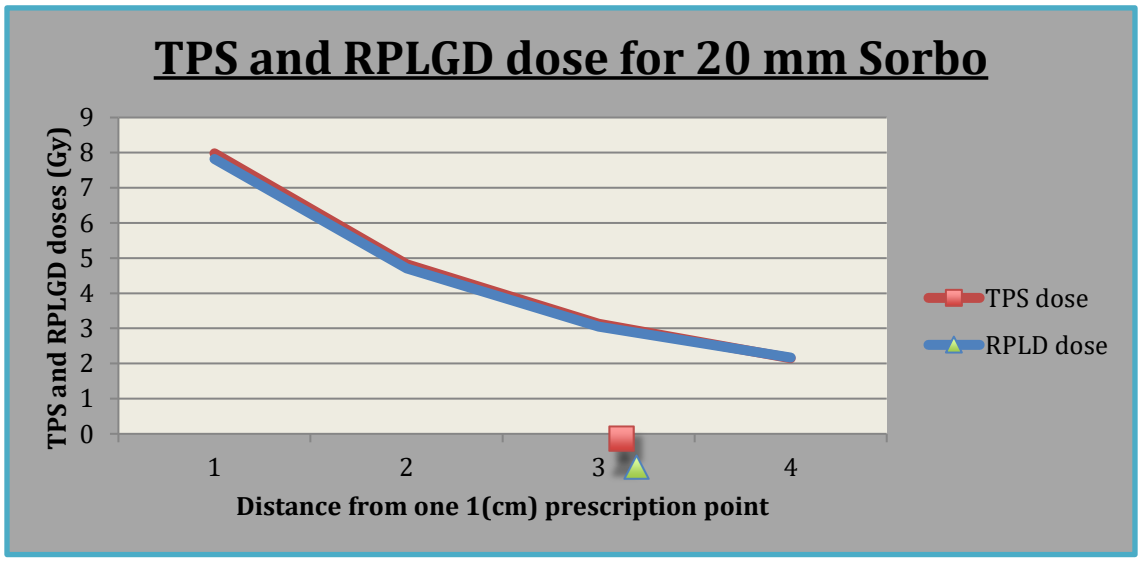


Figure 4.5: Comparison of the doses calculated by the TPS to those measured by the RPLGDs around a 20 mm sorbo applicator.

The percentage difference between TPS and RPLGD was 0.02% at 0.5 cm from the surface of the sorbo applicator.

4.6. Absorbed dose (Gy) TPS brachytherapy and RPLGD for ring tube and IU 6 cm applicators

Table 4.7 and table 4.8 and **figure 4.6 to 4.7** provide percentage error results of the agreement between the measured RPLGD's and the corresponding plane from the TPS exported treatment dose. The ring and IU results are shown on table 4.6 while the table 4.7 shows the ovoids and IU.

Table 4.6: Comparison of the doses calculated by the TPS to those measured by RPLGDs for 26 ring and 6 cm IU applicator

Distance from the centre of the applicator	TPS brachy dose (Gy)	RPLGD dose (Gy)	+/- % Error
2	7.921	7.71	2.74
3	4.74	4.61	2.73
4	2.975	2.96	0.52
5	2.113	2.17	2.79
6	1.459	1.28	14

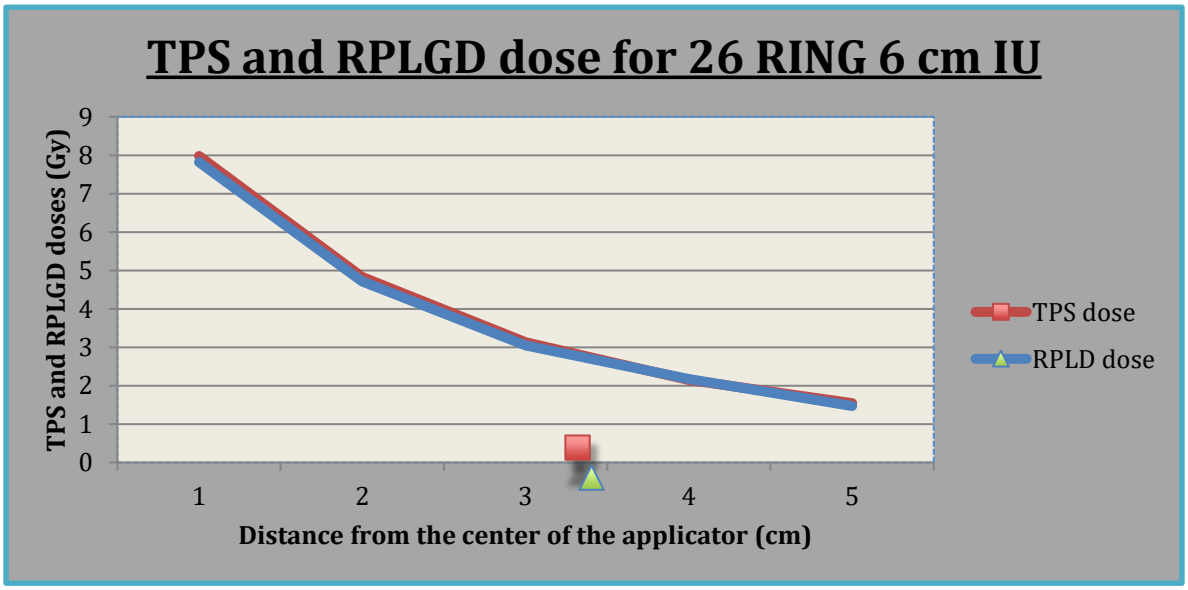


Figure 4.6: Comparison of the doses calculated by the TPS to those measured by the RPLGDs for 26 ring tube and 6 cm IU applicator

4.7. Absorbed dose (Gy) TPS brachytherapy and RPLGD for ovoids tubes and IU 6 cm applicators

Table 4.7: Comparison of the doses calculated by the TPS to those measured by RPLGDs for Ovoids and 6 cm IU applicator

Distance from the centre of the applicator	TPS brachy dose (Gy)	RPLGD dose (Gy)	% Error
2	7.981	7.82	2.07
3	4.827	4.71	2.52
4	3.129	3.05	2.48
5	2.151	2.17	1.05
6	1.546	1.47	5.16

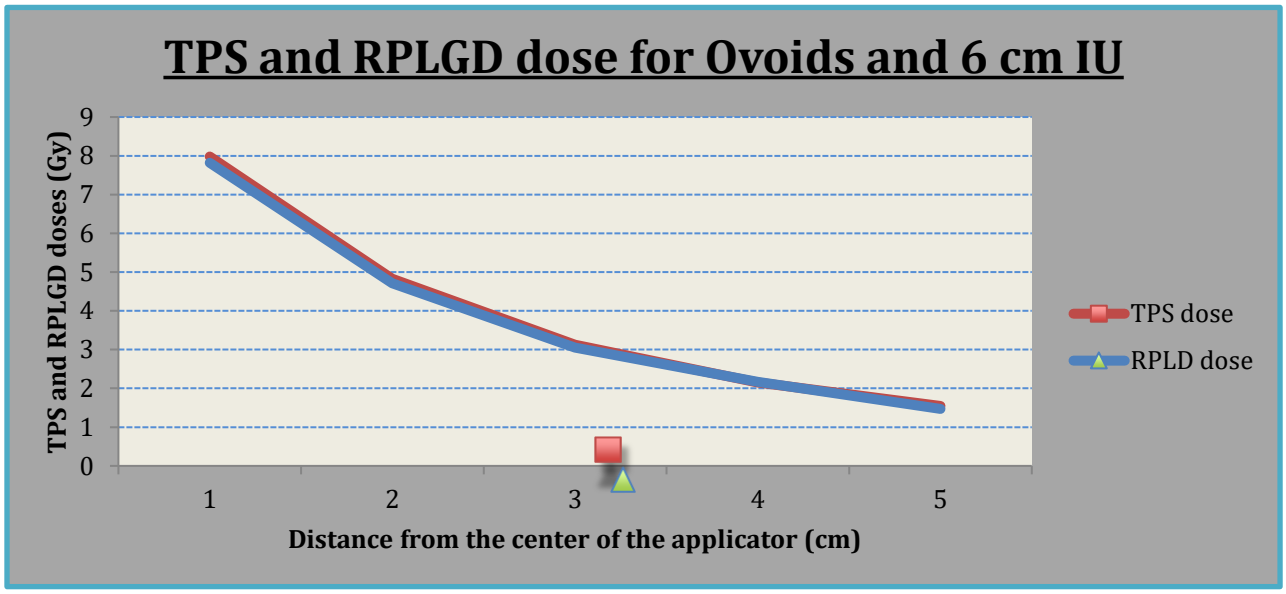


Figure 4.7: Comparison of the doses calculated by the TPS to those measured by the RPLGDs for ovoids tube and 6 cm IU tube applicator

4.8. Monte Carlo technique

Table 4.9 and 4.10 and **figure 4.8** presents the results of Monte Carlo calculations for ring and IU, and ovoids and IU respectively. Table 4.11 and 4.12 compares the dose delivered to a water phantom using TPS, RPLGD's and Monte Carlo calculations.

Table 4.8: The dose calculated by TPS and MC for R26 and IU of 6 cm tube showing the left and right-side applicators.

	Left side of the applicator set						**Right side of the applicator set**					
	7 cm	6 cm	5 cm	4 cm	3 cm	2 cm	2 cm	3 cm	4 cm	5 cm	6 cm	7 cm
MC Doses (Gy)	1.17	1.53	2.08	3.01	4.63	7.96	8	4.73	3.07	2.10	1.52	1.13
TPS Doses (Gy)	1.10	1.456	2.113	2.975	4.740	7.921	7.932	4.742	3.002	2.114	1.470	1.11

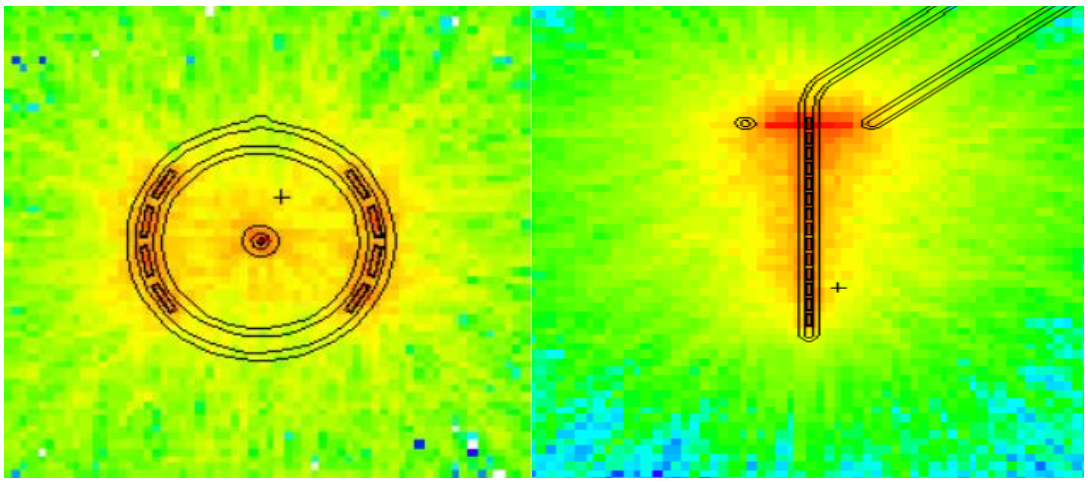


Figure 4.8: The image shows the MC doses for ring and 6 cm IU tube applicator

Table 4.9: The dose calculated by TPS and MC for Ovoids and IU of 6 cm tube showing the left and right-side applicators.

	Left side of the applicator set					Right side of the applicator set				
	6 cm	5cm	4 cm	3 cm	2 cm	2cm	3 cm	4 cm	5 cm	6 cm
MCDoses (Gy)	1.50	2.02	2.90	4.57	7.71	8	4.74	3.08	2.13	1.52
TPS Doses (Gy)	1.546	2.151	3.129	4.827	7.981	7.992	4.750	3.092	2.160	1.567

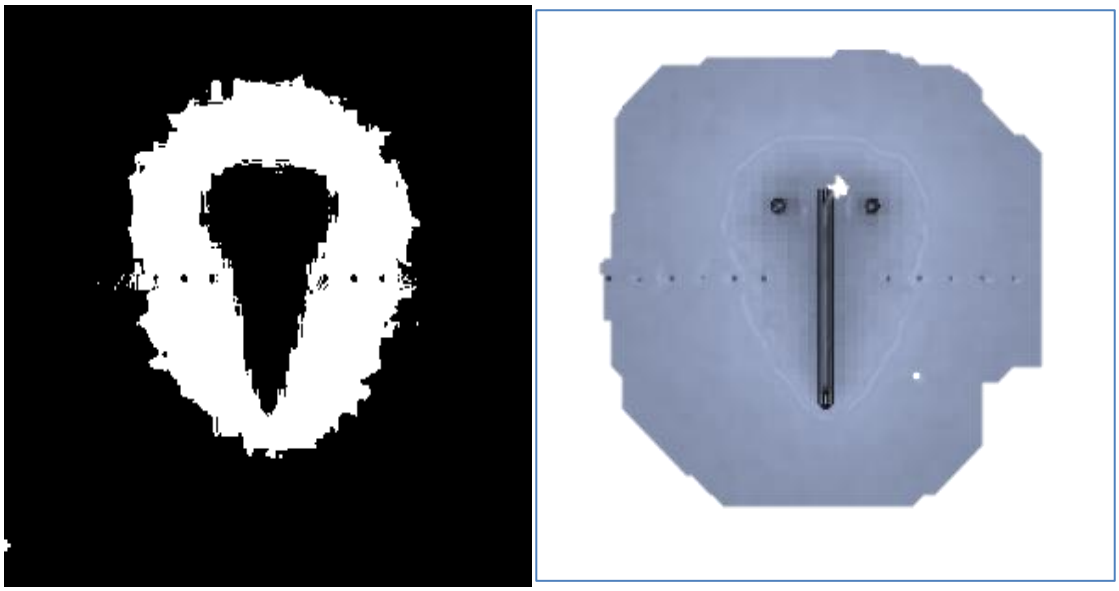


Figure 4.9: The 2-dimensional view of the dose distribution modelled by the MCNP code normalised at 20 mm radial distance from the center of the applicator.

Table 4.10: The comparison of measured and calculated doses at different distances from point A for the 26 cm diameter ring and 6 cm IU

Measurement points (cm)	RPLG measurements (Gy)	Brachy TPS measurements (Gy)	Monte Carlo Simulation (Gy)
2	7.71	7.92 (+/- 2.70 %)	8.02 (-4.02)
3	4.61	4.74 (+/- 2.70 %)	4.56 -1.08
4	2.96	2.98 (+/- 0.52%)	3.03 (-2.36)
5	2.17	2.11 (+/- 2.79%)	2.07 -7.4
6	1.28	1.46 (+/- 14.0 %)	1.6 (-25.0)

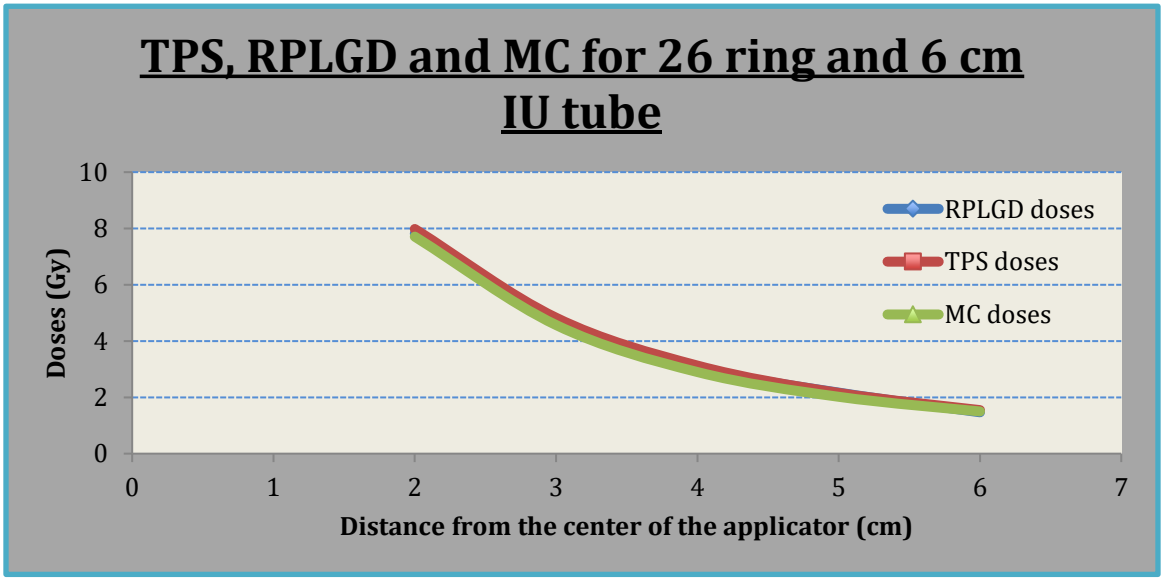


Figure 4.10: Comparison of the doses calculated by the TPS and (MC) to those measured by the RPLGDs for 26 ring tube and 6 cm IU applicator.

Table 4.11: The comparison of measured and calculated doses for ovoids and 6 cm IU

Measurement points (cm)	RPLG measurements (Gy)	Brachy TPS measurements (Gy)	Monte Carlo Simulation (Gy)
2	7.82	7.981 (+/- 2.06 %)	7.71 (+/-1.41 %)
3	4.71	4.827 (+/- 2.50 %)	4.57 (+/-2.97 %)
4	3.05	3.129 (+/- 0.52 %)	2.9 (+/-4.92 %)
5	2.17	2.151 (+/- 0.88 %)	2.02 (+/-6.91 %)
6	1.47	1.547 (+/- 5.24 %)	1.5 (+/-2.04%)

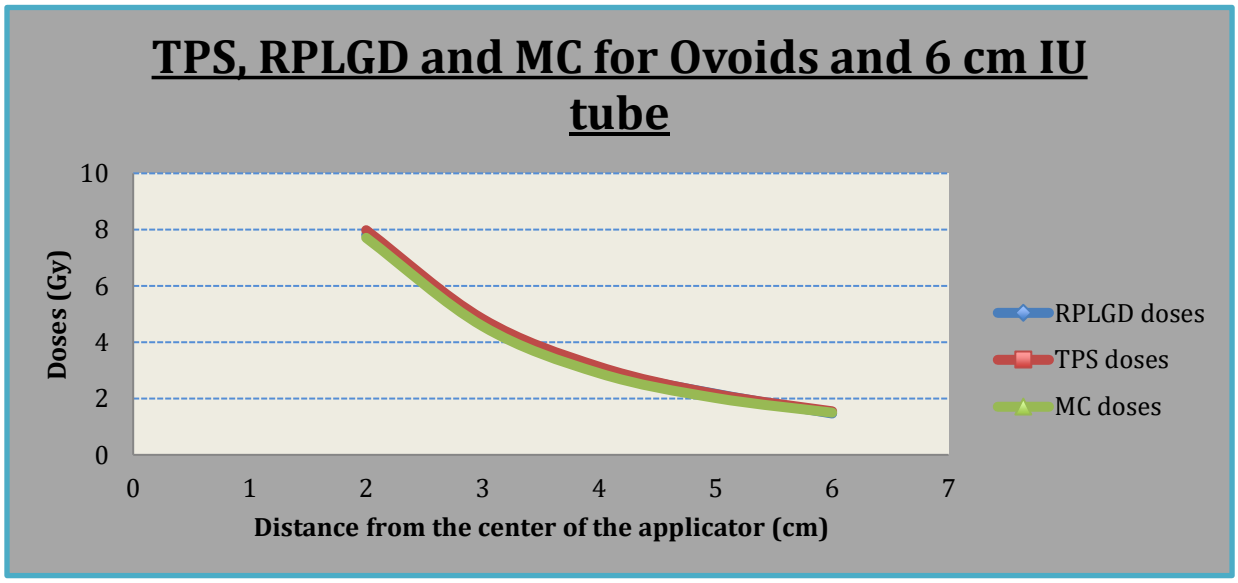


Figure 4.11: Comparison of the doses calculated by the TPS and (MC) to those measured by the RPLGDs for Ovoids tube and 6 cm IU applicator.

The RPLG dosimeters dose was in good agreement with treatment-planning doses and Monte Carlo simulated doses. From point "A" to point "B" the variation was less than 3%. 6 cm shows under response of glass dosimeters compared to TPS. This is not corresponding

with the previous studies done by Palmer et al. (2013b), using Gafchromic EBT3 film. They were high discrepancy found at doses less than or around 1 Gy.

BrachyVision TPS is using TG-43 parameters for dose calculations. The percentage difference in TG-43 are highly affected by energy of the photons emitted from brachytherapy sources, and the amount of missing tissue (the phantom size) Williamson et al., 1995. Several researchers have studied the phantom size as an important point in brachytherapy dosimetry study. Williamson et al., 1995. Showed 5%- 10% differences of distances greater than 5 cm from Ir-192 source compared with treatment planning system based on TG-43 algorithm.

The results of this work have shown RPLG dosimeters capable of dose distribution measurements for the purpose of quality control, commissioning checks, and a dosimetric audit from point “A” to point “B”.

4.9. Uncertainty analysis

A criterion for the determination of an out of tolerance result in end-to-end brachytherapy doses requires the establishment of the overall uncertainty budget as shown on table 4.13. This includes RPLD dosimetry within a 30 x 30 x 30 cm^3 water phantom, as well as the uncertainty of the TPS TG-43 calculation, and HDR treatment dose delivery. An estimate using simple quadrature sum of different components of the uncertainty combined were calculated.

Table 4.12: The uncertainty budget for the experimental determination of the agreement between TPS planned and designed phantom glass dosimeter dose

Component	Source of uncertainty	Type (k=1)
Applicator reconstruction on TPS MCNP calculation HDR treatment dose delivery RPLG dosimetry	Applicator position in CT data set Monte Carlo derived Source strength Source dwell position Co-60 calibration RPLG calibration RPLG position Reproducibility Sensitivity	B 2.61% B 0.5% A 0.5% B 1% B 1% B 1.5% B 0.5% A 0.25% A 0.28%
		3.78% Combined uncertainty

CHAPTER FIVE

Conclusions

End-to-end brachytherapy dosimetry checks were conducted at CMJAH. A phantom was designed using a CAD software such that RPLGDs could be positioned accurately at the level of point "A", which is 2 cm to the left and right of an IU tube and 2 cm superior to the surface of an ovoid or the cover of a ring applicator. Additional RPLGDs could be placed parallel to the dosimeter at point "A" at 1 cm intervals up to 7 cm laterally.

The phantom was designed in such a way that it can accommodate all the applicators that were used in this study. The planning system doses were compared with the measurements using the RPLGDs and Monte Carlo simulated doses.

RPLGD methods have been successfully used for the measurement of dose distributions in high dose rate brachytherapy for end-to-end audit purposes. The phantom was designed in house, built and evaluated for use at CMJAH for end to end brachytherapy dosimetry audit tests. The phantom securely holds typical rigid gynaecological HDR treatment applicator sets and glass dosimeters at fixed positions from the applicator. GE CT scans of the phantom with the applicators were taken and these were exported to the brachytherapy treatment-planning system. The applicators were reconstructed on the images and plans were created, using the standard clinical protocols at CMJAH. 8 Gy was prescribed to point A on the TPS and dose measurements were taken. RPLGDs dose readings were used for comparison to Monte Carlo and TPS calculated doses.

Auditing brachytherapy allows an independent check to be made, such as dose delivery or TPS procedures. Brachytherapy treatment is a well-known procedure in South Africa, but currently no national dosimetry audit of brachytherapy is available. The project was successful achieved in performing an end to end HDR gynaecological brachytherapy auditing at CMJAH.

Dosimetry audits are very important to reduce higher possibility of organs at risk to receive the unintended doses, which could cause harm and increase complications to the patient. Dosimetry audits are intended to improve accuracy, minimise potential errors, avoid litigation and improve patient care. Future research could be rectal wall in-vivo dosimetry calibration using RPLGDs in gynaecological HDR brachytherapy.

REFERENCES

1. Alireza, N., & Mesbahi, A. (2010). Application of Monte Carlo calculations for validation of a treatment planning system in high dose rate brachytherapy. Elsevier , 14, 200–204.
2. Andreo, P. (1991). Monte Carlo techniques in medical radiation physics. Journal of Physics, Biology and Medicine , 36, 861-920, 4502-4514.
3. Ballester, F., Granero, D., Perez-Calatayud, J., Casal, E., Agramunt, S., & Cases, R. (2005). Monte Carlo dosimetric study of the BEBIG Co-60 HDR source. Physics in Medicine and Biology , 50, 309-316.
4. Ballester, F., Puchades, V., Lluch, J.L., Serrano-Andrés, M.A., Limami, Y., Pérez-Calatayud, J., et al. (2001). Technical note: Monte-Carlo dosimetry of the HDR 12i and Plus 192 Ir sources. Medical Physics , 28, 2586–91.
5. Borg, J., & Rogers, D. (1999). Monte Carlo Calculations of Photon Spectra in Air from 192 Ir Sources, NRC Report PIRS-629r. Ottawa, Ontario, Institute for National Measurement Standards National Research Council.
6. Burns, G., & Reaside, D., (1989). The accuracy of single-seed dose superposition for I-25 implants. Medical Physics , 16, 627-631.
7. Carrier, J., D'Amours, M., Verheagen, F., Reniers, B., Martin, A., Vigneault, E., et al. (2007). Postimplant dosimetry using a Monte Carlo dose calculation engine: A new clinical standard. International Journal of Radiation Oncology Biology and Physics , 68, 1190-1198.
8. Chibani, O., Williamson, J., & Todor, D. (2005). Dosimetric effects of seed anisotropy and interseed attenuation for 103Pd and 125I prostate implants. Medical Physics , 32, 2557-2566.
9. Gifford, K., Horton, J.J., Pelloski, C., Jhingran, A., Court, L., & Mourtada, F.E. (2005). A three dimensional computed tomography assisted Monte Carlo evaluation of ovoid shielding on the dose to the bladder and rectum in intracavitary radiotherapy for cervical cancer . International Journal of Radiation Oncology Biology and Physics , 63, 615-621.
10. Granero, D., Perez-Calatayud, J., & Ballester, F. (2007). Technical note: Dosimetric study of a new Co-60 source used in brachytherapy. The International Journal of Medical Phyiscs Research and Practice , 34 (9), 3485-3488.

11. Guerrero, R., Almansa, J.F., Torres, J., & Lallena, A.M. (2014). Dosimetric characterization of the 60Co BEBIG Co0.A86 high dose rate brachytherapy source using PENELOPE. Physica Medica , 960-967.

12. Harrison, R.L. (2010). Introduction To Monte Carlo Simulation. AIP Conference Proceedings 1204,17 (https://doi.org/10.1063/1.3295638.

13. Kirov, A., Williamson, J., Meigooni, A., & Zhu, Y. (1996). TLD, diode and Monte Carlo dosimetry of an 192 Ir source for high dose-rate brachytherapy. Physics in medicine and biology. , 40 (12), 2015-36.

14. Krishnaswamy, V., & Hale, J. (1971). Calculation of the dose distribution about californium-252 needles in tissue. Radiology , 98 (1), 155-160.

15. Landry, G., Rivard, M.J., Williamson, J.F., & Verhaegen, F. (2013). Monte Carlo methods and applications for Brachytherapy Dosimetry and Treatment Planning. In J. Seco, & F. Verhaegen (Eds.), Monte Carlo Techniques in Radiation Therapy (pp. 125-139). Madison: Taylor and Fransis Group LLC.

16. Lemaréchal, Y., Bert, J., Falconnet, C., Després, P., Valeri, A., Schick, U., et al. (2015). GGEMS-Brachy: GPU GEant4-based Monte Carlo simulation for brachytherapy applications. Physics in Medicine and Biology , 60 (13), 4987-5006.

17. Li, Z., Das, R., DeWerd, L., Ibbott, G., Meigooni, A., Perez, J.C., et al. (2007). Dosimetric prerequisites for routie clinical use of photon emitting brachytherapy sources with average energy higher than 50 keV. Medical Physics , 34, 37-40.

18. Naeem, H., Chen, C., Zheng, H., Ruifen, C., Xi, P., Liqin, H., et al. (2016). Investigation of Dosimetric Parameters of 192Ir MicroSelectron v2 HDR Brachytherapy Source Using EGSnrc Monte Carlo Code, University of science and Technology of China, Hefei, Anhui, 230027, China..

19. NuDat. (2008). National Nuclear Data Center, Brookhaven National Laboratory. Retrieved July 10, 2018 from http://www.nndc.bnl.gov/nudat2/

20. Perez-Calatayud, J., Ballester, F., Das, K.R., Dewerd, L., Ibbott, G., Meigooni, S.A., et al. (2012). Dose calculation for photon-emitting brachytherapy sources with average energy higher than 50 keV: Report of the AAPM and ESTRO. Medical physics , 39, 2904-29.

21. Poon, E., & Verheagen, F. (2009). Development of a scatter correction tecnique and its application to HDR 192Ir multicatheter breast brachytherapy. Medical Physics , 36, 3703-3713.

22. Poon, E., Reneirs, B., Devic, S., Vuong, T., & Verhegen, F. (2006). Dosimetric characterisation of a novel intracavitary mold applicator for 192Ir high dose rate endorectal brachytherapy treatment. Medical Physics , 33, 4515-4526.

23. Rivard, M.J., Coursey, B.M., DeWerd, L.A., Hanson, W.F., Huq, M., Ibbott, G.S., et al. (2004). Update of AAPM Task Group No.43 Report: A revised AAPM protocol for brachytherapy dose calculations. American Association of Medical Physicists in Medicine , 31 (3), 633-674.

24. Valicenti, R., Kirov, A., Meigooni, A., Mishra, V., Das, R., & Williamson, J. (1995). Experimental validation of Monte Carlo dose calculations about a high intensity Ir-192 source for pulsed dose rate brachytherapy. Medical Physics , 22, 821-829.

25. Williamson, J., & Z, L. (1995). Monte Carlo aided dosimetry of the microselectron pulsed and high dose-rate 192Ir sources. Journal of Medical Physics , 22 (2), 809–819.

26. X-5 Monte Carlo Team MCNP. (2003). MCNP — A General Monte Carlo N-Particle Transport Code, Version 5 Volume II: User's Guide. Los Alamos: Los Alamos National Laboratory.

27. Araki, F., Moribe, N., Shimonobou, T., & Yamashita, Y. (2004). Dosimetric properties of radiophotoluminescent glass rod detector in high-energy photon beams from a linear accelerator and Cyber-Knife. Medical Physics, 31, 1980–1986.

28. Hsu, S.M., Yang, H.W., Yeh, T.C., Hsu, W.L., Wu, C.H., Lu, C.C., Huang, D.Y. C. (2007). Synthesis and physical characteristics of radiophotoluminescent glass dosimeters. Radiation Measurement, 42, 621–624.

29. Hsu, S.M., Yeh, S.H., Lin, M.S., & Chen, W.L. (2006). Comparison on characteristics of radiophotoluminescent glass dosemeters and thermoluminescent dosemeters. Radiation Protection Dosimetry, 119(1–4), 327–331.

30. Huang, D.Y.C., & Hsu, S.M. (2017). Radio-photoluminescence glass dosimeter (RPLGD).Retrieved23October2017http://cdn.intechopen.com/pdfs/23935/InTech Radio_Photoluminescence_glass_dosimeter_rplgd_.pdf.

31. Mizuno, H., Kanai, T., Kusano, Y., Ko, S., Ono, M., Fukumura, A., & Ishikura, S. (2008). Feasibility study of glass dosimeter postal dosimetry audit of high-energy radiotherapy photon beams. Radiotherapy and Oncology, 86(2), 258–263.

32. Rah, J., Hong, J., Kim, G., Kim, Y., Shin, D., & Suh, T. (2009a). A comparison of the dosimetric characteristics of a glass rod dosimeter and thermoluminescent dosimeter for mailed dosimeter. Radiation Measurement, 44, 18–22.

33. Rah, J., Shin, D., Jang, J., Kim, M., Yoon, S., & Suh, T. (2008). Application of glass rod detector for the output factor measurement in the CyberKnife. Applied Radiation and Isotopes, 66, 1980–1985.

34. Rah, J.E., Kim, S., Cheong, K.H., Lee, J.W., Chung, J.B., Shin, D.O., Suh, T.-S. (2009b). Feasibility study of radiophotoluminescent glass rod dosimeter postal dose intercomparison for high energy photon beam. Applied Radiation and Isotopes, 67,324–328.

35. Son, K., Jung, H., Shin, S.H., Lee, H.H., Kim, M.S., Ji, Y.H., & Kim, K.B. (2011). Evaluation of the dosimetric characteristics of a radiophotoluminescent glass dosimeter for high-energy photon and electron beams in the field of radiotherapy. Radiation Measurement, 46(10), 1117–1122.

36. Wesolowska, P.E., Cole, A., Santos, T., Bokulic, T., Kazantsev, P., & Izewska, J. (2017). Characterization of three solid state dosimetry systems for use in high energy photon dosimetry audits in radiotherapy. Radiation Measurement, 106, 556–562.

37. Palmer AL, Bradley DA, Nisbet A. (2014). Dosimetric audit in brachytherapy. Br J Radiol ; 87: 20140105.

38. Amelie R, Jack L.M. (2007). TLD mailed dosimetry. Radiotherapy and Oncology ; 86-93.

39. Critically ill received wrong radiation therapy due to human errors: review. 12 September 2003. [about 1 pp.]. Cited 21 January 2014.

40. The ASAHI SHIMBUN. Asia & Japan Watch internet media site. Hospital delivers radiation to wrong spots in 100 cancer treatment cases. [about 1 pp.].

41. AGS TECHNO GLASS., LTD RPL Glass Dosemeter/ small element system Technical Guide 2008.

42. Annette H, Duncan JB. (2013). Comparison of TLD calibration methods for 192 Ir dosimetry. Journal of Applied Clinical Medical Physics, 14(1).

43. [7] William RH. (2013). Comprehensive Brachytherapy, Physical and Clinical Aspects. Taylor and Francis Group, LLC Series Editor

44. European Society for Therapeutic Radiology and oncology. A practical Guide to Quality Control of Brachytherapy Equipment ESTRO Booklet no. 8 2004; Mounierlaan 83/12- 1200 Brussels.

45. Eckert & Ziegler BEBIG GmbH. Urgent Field Safety Notice reference 2014LCT82. Mispositioning [sic] of source. Eckert & Ziegler Bebig GmbH, Berlin, Germany, 17 March 2014. CRC/ Taylor & Francis Group, Boca Roca Raton, FL, 2013.

46. Araki, F., Moribe, N., Shimonobou, T., Yamashita, Y., 2004. Dosimetric Properties of Radiophotoluminescent glass rod detector in high-energy photon beams for linear Accelerator and Cyber-knife. Med. Phys. 31, 1980e1986.

47. Rah, J., Shin, D., Jang, J., Kim, M., Yoon, S., Suh, T., 2008a. Application of a Glass Rod Detector for the output factor measurement in the CyberKnife. Appl. Radiat. Isot 66, 1980e1985.

48. Palmer AL, Bradley DA, Nisbet A. (2014). Dosimetric audit in brachytherapy. Br J Radiol 2014; 87: 20140105.

49. Amelie R, Jack L.M, TLD mailed dosimetry. Radiotherapy and Oncology 2007; 86-93 www.thegreenjournal.com

50. Critically ill received wrong radiation therapy due to human errors: review. 12 September 2003. [about 1 pp.]. Cited 21 January 2014.

51. The ASAHI SHIMBUN. (2003). Asia & Japan Watch internet media site. Hospital delivers radiation to wrong spots in 100 cancer treatment cases.[about 1 pp.].

52. AGS TECHNO GLASS., LTD RPL Glass Dosemeter/ small element system Technical Guide 2008.

53. Annette H., Duncan JB., (2013). Comparison of TLD calibration methods for 192 Ir dosimetry. Journal of Applied Clinical Medical Physics, 14(1).

54. Yokota R., Muto Y., (1971). Silver-activated phosphate dosimeter glasses with low energy dependence and higher sensitivity. Health phys. 20, 662.

Ethics clearance

UNIVERSITY OF THE WITWATERSRAND, JOHANNESBURG

HUMAN RESEARCH ETHICS COMMITTEE (MEDICAL)

Ref: W-CBP-170927-1 27/09/2017

TO WHOM IT MAY CONCERN:

Waiver: This certifies that the following research does not require clearance from the Human Research Ethics Committee (Medical).

Investigator: Mr L. Ntombela (student no. 818411).

Project title: Radiopholotoluminescence Glass (RPLG) Dosimetry end to end Audit of High Dose Rate Gynaecological Brachytherapy inn Charlotte Maxeke Johannesburg Academic Hospital

Reason: This study will be done using information in the public domain. There are no human participants.

UNIVERSITY OF THE WITWATERSRAND
OFFICE OF THE DEPUTY VICE CHANCELLOR RESEARCH
27 SEP 2017
RESEARCH OFFICE HREC (Medical)
JOHANNESBURG

Professor Clement Penny

Co-Chair: Human Research Ethics Committee (Medical)

Copy – HREC (Medical) Secretariat: Zanele Ndlovu, Rhulani Mkansi, Lebo Moeng.

Research Office Secretariat: Faculty of Health Sciences, Phillip Tobias Building, 3rd Floor, Office 302, Corner York Road and 29 Princess of Wales Terrace, Parktown, 2193 Private Bag 3, Wits 2050 I **T**+27 (0)11-717-1234/2656/2700/1252 **E**: Lebo.Moeng@wits.ac.za I **Office E** HREC-Medical.ResearchOffice@wits.ac.za IWebsite: www.wits.ac.za/research/about-our-research/ethics-and-research-integrity/